Assessment of IDPS VIIRS Cloud Products

and

Recommendations for EOS-era Cloud Climate Data Record Continuity

The Suomi NPP Science Team for Clouds

Steven Platnick[1,✧], Steven A. Ackerman[2], Bryan A. Baum[2], Andrew K. Heidinger[2,3], Robert E. Holz[2], Michael D. King[4], W. Paul Menzel[2], Shaima Nasiri[5], Elisabeth Weisz[2], Ping Yang[5]

[1] NASA Goddard Space Flight Center, Greenbelt, MD
[2] CIMSS/SSEC, University of Wisconsin-Madison, Madison, WI
[3] NOAA NESDIS/STAR, College Park, MD
[4] LASP, University of Colorado, Boulder, CO
[5] Texas A&M University, College Station, TX

✧ Cloud Team Lead

March 19, 2013

WHO WE ARE: THE SUOMI NPP SCIENCE TEAM FOR CLOUDS

The team consists of three separately funded investigations, each focusing on a specific suite of VIIRS cloud data records and/or related algorithms issues. The teams are listed below (in order of PI, Co-I, and key collaborators and science support staff). Each individual's product evaluation emphasis is given and, if applicable, key writing responsibilities/contributions for the report. Acronyms are defined in Appendix C.

- Cloud mask, cloud thermodynamic phase, cloud-top parameters, cloud optical properties:

  Steven Platnick (COP, Sect. 1, 4, 5.1, 5.3 & 6), Steven A. Ackerman (Cloud Mask/Phase, Sect. 2), Andrew K. Heidinger (CTP, Sect. 3 & 2, PATMOS-x, VIIRS_AWGMOD), Robert E. Holz (co-location, COP gridding code and visualization, Sect. 1, 3 & 4, PEATE liaison), Michael D. King (COP), Galina Wind (MOD06 and VIIRS_AWGMOD), Nandana Amarasinghe (COP LUTs), Rich Frey (Cloud Mask/Phase).

- Cloud-top parameters and use of CrIS observations:

  Bryan A. Baum (CrIS_CTP_DR, Sect. 5.2 & 3), W. Paul Menzel (CrIS_CTP_DR), Elisabeth Weisz (CrIS_CTP_DR algorithm), Nadia Smith (CTP gridding code and analysis).

- Ice cloud radiative model evaluation

  Ping Yang, Shaima Nasiri (Sect. 4.3.1)

Table of Contents

Executive Summary i

1. Introduction and Assessment Overview 1

1.1 Overview of Instruments and Products 1
1.2 Evaluation Philosophy 2
1.3 VIIRS IDPS Cloud Products and Mapping to MODIS Heritage Products 6
1.4 Overview of Atmosphere PEATE Data Set Production and Tools 6
1.5 Comments on Algorithm Continuity and Trend Detection 7
1.6 Annual Cycle of IDPS IP Cloud Products 10

2. VIIRS Cloud Mask and Thermodynamic Phase (VCM) 12

2.1 Comparison of Key Algorithm Approaches: IDPS vs. MODIS 12
2.2 Evaluation Methodologies 12
2.3 Evaluation Results 13
2.4 Conclusions 21

3. Cloud Top Parameters (CTP) 22

3.1 Comparison of Key Algorithm Approaches 22
3.2 Evaluation Methodologies 24
3.3 Evaluation Results 25
3.4 Conclusions 33

4. Cloud Optical Parameters (COP) 34

4.1 Comparison of Key Algorithm Approaches: IDPS vs. MODIS 34
4.2 Evaluation Methodologies 35
4.3 Evaluation Results 36
4.3.1 Ice LUT comparisons 36
4.3.2 Retrieval comparisons 39
4.4 Conclusions 41

5. Recommendations for the Way Forward 42

5.1 Achieving Cloud Data Record Continuity Across the MODIS/VIIRS Instrument Record 42
5.2 Improving Cloud Top Parameters/Phase with CrIS and VIIRS Observations 43
5.3 Development of Level-3 Gridded Products 47

6. Summary 47

Appendix A. References 49

Appendix B. Overview of Suomi NPP Cloud Team Objectives and Activities 54

Appendix C. Key Acronyms 56

Executive Summary

Among the atmospheric properties being monitored and examined from space, clouds are especially important. They are the strongest modulator of the shortwave and longwave radiative budget, are of obvious importance to the hydrological cycle. Further, their feedbacks in response to global warming are not well understood, constituting the largest source of inter-model uncertainty in climate sensitivity [e.g., *Dufresne and Bony*, 2008]. Knowledge of cloud properties (extent, height, thermodynamic phase, optical properties, microphysics) and their spatial/temporal variation are crucial to understanding local-scale cloud processes, validating models, and establishing and monitoring cloud climatologies. It is critical to be able to bridge the cloud record established by MODIS into the S-NPP VIIRS timeframe.

Overview

Differences between pixel-level MODIS Level-2 cloud product and VIIRS Intermediate Products (IPs) and Environment Data Records (EDRs) are ultimately related to a combination of two primary factors: (1) differences between the MODIS and VIIRS instruments, and (2) differences in the geophysical algorithms, including radiative models, ancillary data sets, and QA filtering of pixels. De-convolving these two factors is challenging.

With regard to the sensors, several key spectral channels are absent on VIIRS (water vapor and 13-14 μm CO_2 channels), there is a significant change in the spectral location of the 2.1 μm shortwave infrared channel used for MODIS cloud microphysical retrievals, and there are differences in pixel spatial resolution vs. scan angle as well as swath width.

With regard to algorithms, it is as important to have a consistent algorithm for data record continuity, including forward radiative models and ancillary data sources, as it is to have instruments with similar measurement information content. While MODIS and VIIRS instrument differences are a given, geophysical algorithm differences can be eliminated (or at least minimized) by the use of a consistent algorithm applied to both sensors.

For cloud-top and optical property products, we have ported a version of the upcoming MODIS Collection 6 (C6) cloud optical property algorithm (product MOD06) to VIIRS, in combination with the GOES-R Algorithm Working Group (AWG) cloud-top property algorithm that utilizes the same IR channels available on VIIRS. Enabling these algorithms to run on the VIIRS spectral channel set allows for direct and meaningful comparisons with algorithms provided by Northrop Grumman Aerospace Systems (NGAS) and implemented by the VIIRS Interface Data Processing Segment (IDPS). This eliminates instrument-related differences and provide a hybrid heritage reference algorithm that can be used for evaluation of VIIRS EDRs. It also provides an algorithm pathway for enabling a consistent MODIS/VIIRS cloud data record (albeit, inferior to MODIS) that can be run on both instruments and thereby bridge the instrument records for multi-decadal climate studies. The use of CrIS observations to provide MODIS-like CO_2 slicing information for improving cloud-top properties has also been investigated.

Analysis

The team's most recent analysis of IDPS cloud products were for those generated following a Look-up Table update delivered by NGAS in August 2012. The evaluation in this report

focuses on IDPS cloud IPs and/or EDRs for the month of September 2012 as well as seasonal changes in cloud properties. Using both team and Atmosphere PEATE aggregation codes developed for this study, evaluations included monthly statistical comparisons between the IDPS products and: (1) the archived MODIS Aqua Collection 5 (C5) Level-3 cloud product (MOD08); (2) a Collection 6 (C6) test code run at the Atmosphere PEATE on Aqua MODIS data, and (3) the hybrid AWG/MOD06 algorithm mentioned above. In addition, pixel-level evaluations have been done for the VIIRS cloud mask (VCM) and cloud-top property products by co-location with the CALIOP lidar aboard CALIPSO in the NASA afternoon constellation (A-Train). Direct comparisons against co-located MODIS Aqua retrievals have also been done. From the processing infrastructure perspective, the Atmosphere PEATE acquired the needed IDPS and A-Train products and processed team algorithms. The PEATE also provided a number of visualizations and tools that enabled the analysis in this report.

Conclusions

Instrument measurement (information content) continuity is a necessary but not sufficient element for bridging a climate quality data record. Consistent algorithms are also required (including forward radiative models, ancillary data sets, filtering, etc.). The implicit JPSS paradigm inherited from the NPOESS program is that instrument continuity alone is sufficient. As a result, and as substantiated in the body of this report, we conclude:

1. The pixel-level IDPS IP cloud products evaluated in this report are outside the bounds of acceptable retrieval differences needed for climate analysis [*Ohring et al.*, 2005; Sect. 1.5] relative to either the standard MODIS products or the VIIRS/CrIS evaluation products processed by the team. Therefore, in our opinion, the IDPS products are incapable of continuing the MODIS cloud climate data record into the NPP VIIRS timeframe.
2. While MODIS measurements have more inherent cloud information content, suitably designed consistent algorithms that can be run on both VIIRS and MODIS measurements have been shown to provide a pathway for establishing a cloud data record that can bridge the EOS/NPP imager instrument record. Further, inclusion of CrIS observations to supplement the absence of VIIRS CO_2 slicing channels has shown promise.
3. It is unclear what aggregation choices have been made in the generation of ~5 km scale EDRs from the IP products that are more directly comparable with MODIS Level-2 products and other (future) algorithms run on VIIRS measurements. This results in a further disconnect between EOS and archived IDPS products since only EDRs are stored in the NOAA CLASS facility.
4. As is well-known, JPSS requirements do not include reprocessing by the IDPS. Further, integration and use of the stand-alone ADL software has been found to be cumbersome and problematic. Finally, IDPS algorithm codes are written in a manner specific to IDPS interfaces and therefore the porting of these codes to other processing systems will be challenging and time-consuming.
5. As is well-known, JPSS Level 1 requirements do not include the generation of temporal/spatial gridded products (i.e., Level-3 in NASA parlance) that are essential for climate studies as well as many process investigations.

Recommendations

A nearly 13-year data record now exists for MODIS Terra and a 11-year record for Aqua. The climate science community is facing an interruption in the continuity of key global cloud data sets once the EOS Terra and Aqua sensors cease operation. Through NASA's Senior Review process, the Aqua and Terra missions have already been extended three and four times, respectively. While both missions are expected to have enough fuel beyond the 2016 time-frame, the continuity of MODIS cloud data records into the era of the next cloud-focused NASA mission is not possible (e.g., the Decadal Survey's Aerosol Cloud Ecosystems (ACE) mission is perhaps early/mid-2020's at best). Further, the current scope of the ACE mission does not include measurement continuity as an objective. *For these reasons, it is paramount that the VIIRS data be used as effectively as possible to bridge, to the extent possible, cloud data records begun by MODIS in early 2000 after the launch of Terra*.

Due to missing/different spectral channels, VIIRS cloud records will be incapable of directly continuing MODIS records without alternative approaches. To merge a MODIS/VIIRS product, it is critical to have consistent algorithms across the entire record length. By leveraging the team's method for evaluating VIIRS cloud EDRs by porting MODIS/AWG code, we have also demonstrated the means for applying a VIIRS-like code to MODIS that can be used to link the decadal-plus MODIS time series with NPP VIIRS.

Recommendations necessary to continue a subset of the EOS cloud data records for the benefit of the NASA Earth Science Division (ESD) Research & Analysis and Application programs, as well as meeting the needs of the greater climate community, are summarized below. We stress that these recommendations are distinct from operational community needs that are the responsibility of the IDPS; a report from the JPSS Cloud Cal/Val Team has addressed the operational quality of IDPS cloud products [*Heidinger, et al.*, 2012].

1. NASA Algorithms:

    a. *Pixel-level geophysical cloud products (Level-2)*: The algorithm-development undertaken by the team (using common MODIS and VIIRS algorithms that utilize the channel set of the more limited instrument) has demonstrated a pathway for cloud data record continuity that can bridge the MODIS and VIIRS sensors. The use of CrIS algorithms to account for the loss of VIIRS CO_2 shows promise. It is recommended that ESD support the development and processing of such algorithms.

    b. *Gridded cloud products (Level-3)*: The MODIS Atmosphere Team experience is that retrieval statistics can be extremely sensitive to aggregation choices, and that the development of a robust, flexible, and maintainable aggregation code is not the relatively trivial task it is often thought to be. It is recommended that ESD support the development of gridded products. It is further recommended that at a minimum, the code include aggregation choices that provide compatibility with the MODIS Atmosphere Team's daily, eight-day, and monthly products (MOD08).

    c. *Pixel-level instrument data records (Level-1B)*: In order to have control over the quality of NASA-supported geophysical products, it is critical that ESD provide for its own calibrated and geolocated records.

2. NASA Processing/Reprocessing: It is recommended that ESD support a production system capable of reprocessing NASA-supported NPP data records. The processing system should be tasked to work directly with NASA-funded algorithm developers, and

should be scoped for algorithm development and testing in addition to routine production and distribution.

To minimize additional resources needed to implement the above recommendations, ESD is encouraged to leverage existing instrument, algorithm and processing development efforts from the Senior Review, ROSES, and the NPP line.

The algorithm continuity recommendations are presented as part of a strategic vision for continuing stewardship of critical cloud records that NASA began in the EOS era. It is a strategy based on the team's experience in algorithm product development and climate data analysis, both at the multi-agency (NASA, NOAA) and international (GEWEX, CREW) level. It is also a strategic vision for achieving NASA climate record continuity in a straightforward (low risk) and efficient manner given the likely limited resources available within ESD. The alternate (default) strategy pursued by current and previous NPP science teams has been to provide input to an evolving organization/group that ESD does not manage, in hopes that algorithm changes can be implemented in a way that will eventually converge to the exacting level needed for climate record continuity, and that once there will be maintained for that purpose.

1. Introduction and Assessment Overview

Satellites provide the needed platform for studying the Earth's climate; however, obtaining climate-relevant data from remotely sensing instruments carried by these platforms requires careful planning. There are multiple challenges for developing data sets and measurement strategies to detect climate change. Because of natural variability, typically several missions are required to build the necessary multi-decadal time series. This requires the 'stitching together' of multiple satellite instruments and trying to account for observational differences. The optimum satellite climate data set includes: 1) a set of well characterized and calibrated instruments that provide observations at similar spectral wavelengths/frequencies and are obtained from similar orbits, and 2) common algorithms that transform the observations to geophysical parameters. A change in any one of these requirements will induce uncertainties into the data set and, at best, will require a longer time series for climate change detection with increased uncertainty (see Sect. 1.5). The GEWEX cloud assessment report summarizes the complexities of establishing a cloud climate record [*Stubenrauch et al.*, 2013].

As shown in this report, the S-NPP IDPS cloud products from VIIRS are out of family with the current MODIS cloud products, due to both instrument and/or algorithm differences (depending on the specific product). This impacts both long-term time scale (climate) and short-term uses of the products. However, the S-NPP VIIRS and CrIS sensors are extremely capable and well characterized, and the report demonstrates a pathway for using them to establish high quality cloud products that can bridge the EOS record. These issues are discussed further in Sect. 1.5 and in the evaluation analysis of Sects. 2-4, and in the summary yearly monthly plots of Sect. 1.6.

1.1 Overview of Instruments and Products

The MODIS imagers on Terra and Aqua provides unique spectral and spatial capability for retrieving cloud properties at a 1 km (nadir) pixel-level scale [*Platnick et al.*, 2003; *King et al.*, 2003, 2013]. Relative to previous generation global imagers (e.g., AVHRR), MODIS has a number of additional spectral bands and onboard reflectance calibration. Spectral coverage includes the 0.94 μm and 1.38 μm water vapor bands, and the shortwave infrared (SWIR) 1.6 μm and 2.1 μm window bands that, in addition to an AVHRR heritage 3.7 μm band, provide cloud microphysical information. In the infrared, MODIS includes a set of 13.3–14.2 μm CO_2 sounding bands for high cloud detection and pressure-height retrievals. Native spatial resolution is at 250 m (0.66 μm and 0.86 μm), 500 m (SWIR), and 1 km (all other bands). For some bands (e.g., 0.94 μm, 2.1 μm, 13.3-14.2 μm), this unique capability will remain into the foreseeable future, including the VIIRS and GOES-R ABI time frame.

VIIRS lacks several key spectral channels compared to MODIS (namely, the 6.7, 7.3 μm water vapor channels and 13.3-14.2 μm CO_2 bands used for high cloud properties), and a significant change in the spectral location for the key shortwave infrared band (from 2.13–2.25 μm) used for retrieving cloud effective particle radius that results in a reversal in the relative absorption between liquid water and ice phase particles. In addition, a near-infrared water vapor band (0.94 μm) used for multilayer cloud detection and optical retrieval quality flagging is not available on VIIRS [*Wind et al.*, 2010]. Direct comparison with many MODIS products is therefore futile, e.g., the cloud-top information content of MODIS observations is inherently superior to VIIRS [*Heidinger et al.*, 2010]. With respect to the 2.2 μm window channel location, the shift towards longer wavelengths is not neces-

sarily without merit for phase detection (though not utilized in the VIIRS Cloud Mask (VCM) phase algorithm), but meaningful comparisons with MODIS are unlikely [*Zhang and Platnick*, 2011]. For the same reasons, the direct porting of the MODIS cloud algorithms to the VIIRS instrument to achieve EDR continuity is not possible.

The MODIS cloud products relevant to this proposal are the cloud mask (MOD35 and MYD35 for MODIS Terra and Aqua, respectively) and the MOD06/MYD06 cloud properties product that includes both cloud-top (temperature, pressure, effective emissivity) and optical/microphysical (thermodynamic phase, optical thickness, effective particle radius, water path, multilayer detection) data sets [*Platnick et al.*, 2003; *Ackerman et al.*, 2008; *Frey et al.*, 2008; *Holz et al.*, 2008; *Menzel et al.*, 2008]. MODIS processing streams based on a consistent set of algorithms are referred to as data "collections". Collection 5 (C5) reprocessing began in late spring 2006 and was completed about a year later. The implementation and evaluation of code refinements for Collection 6 (C6) reprocessing is ongoing, with production nominally expected to begin in early 2013. A detailed summary of the Atmosphere Team C6 plans is available at modis-atmos.gsfc.nasa.gov/products_C006update.html. Further mention of MOD35 and MOD06 will implicitly include the Aqua MODIS products unless otherwise stated.

An assessment of the MODIS cloud products has been undertaken by a number of investigators including the MODIS algorithm team. The team has also participated in the GEWEX cloud assessment study [e.g., *Stubenrauch et al.*, 2013]. While such assessments will continue, the uncertainties and/or issues for most of these products are understood and have been documented. Instrument stability, consistent (re-processed) algorithms and ancillary data are recognized as keys to establishing a climate quality data set.

1.2 Evaluation Philosophy

Our primary goal is to evaluate the ability of VIIRS SDRs to continue the EOS MODIS cloud data records. While a subset of such an evaluation includes assessing the suitability of existing Interface Data Processing Segment (IDPS) operational products for continuing MODIS pixel-level (Level-2) records, a higher-level effort is to identify and resolve key issues related to cloud data record continuity from NPP sensors. As such, three evaluation approaches have been pursued by the NPP cloud team and are discussed in this report. A list of these approaches and the rationale behind them follows:

A. Direct evaluation of VIIRS cloud IPs and/or EDRs against MODIS products and other A-Train data.

With similar ascending mode equatorial overpass times as the NASA A-Train constellation, the easiest and most straightforward methodology is to compare global aggregation on a common time and space grid. Unfortunately, the lack of a JPSS Level-3 requirement requires each individual discipline team to develop it's own aggregation code for IDPS products. For the cloud team, several aggregation codes have been developed. In all cases the same aggregation approach and filtering has been used on both the IDPS IP/EDR and the MODIS Level-2 products to the extent that the product's allow.

Suomi-NPP is in an orbit slightly higher than that of the A-Train, and the two tend to fall into alignment for about 1-2 orbits every three days. The Atmosphere PEATE at the University of Wisconsin-Madison is using the computational approach of *Nagle and Holz*

[2009] for collating instantaneous IDPS retrievals with A-Train products (e.g., the CALIOP lidar and other imagers of interest including both VIIRS and MODIS). CALIOP provides extremely high sensitivity to the cloud top and optically thin cirrus [*Winker et al.*, 2007] with a vertical resolution up to 60 meters and an along-track spatial resolution as a high as 330 meters. CALIOP cloud products include cloud thermodynamic phase, optical thickness and cloud boundaries as long as the signal does not attenuate (COT>3).

The comparison approaches described above have been performed with the IDPS and MODIS cloud products summarized in Sect. 1.3.

B. The porting of GOES AWG and MODIS-like algorithms for use with VIIRS SDRs, in order to provide a more representative baseline for assessing the capability of VIIRS IDPS cloud products as well as a pathway to MODIS/VIIRS data record continuity.

The coupled effect of instrument and algorithm differences will prevent unambiguous conclusions to be drawn from the direct comparison of IDPS and MODIS cloud products. Systematic differences that are likely to show up in VIIRS vs. MODIS product comparisons include those related to:

- Instrument differences:
  - Spectral channel differences leading to inherent differences in retrieval information content between the two sensors (e.g., absence of CO_2 slicing channels on VIIRS for cloud-top retrievals, different 2.2 μm window channel position for size retrievals);
  - Calibration and/or instrument artifacts (e.g., optical/ electronic cross-talk, stray light).
- Algorithm differences:
  - Cloud forward radiative models, Look-up Table (LUT) generation gridding and assumptions, and other algorithm details;
  - Use and/or choice of ancillary data sets (surface albedo/emissivity, snow/ice maps, sea ice maps, model clear-sky analyses, etc.);
  - Use of Quality Assurance (QA) or uncertainty analyses to filter retrievals.

Unraveling the various components are difficult and beyond the scope of our proposed activity as well as this report. We proposed an alternate and parallel approach for directly evaluating the IDPS products separate from the instrument by porting MODIS-like algorithms to VIIRS so that both IDPS and the MODIS-like code are run on the same instrument. The evaluation question then becomes: "to what extent do the IDPS products agree with products based on MODIS retrieval algorithms". An advantage of this approach is that it eliminates instrument differences from the comparisons. It also provides a pathways for production of a cloud data record that can provide continuity across the VIIRS/ MODIS time record by using a common algorithm that can be applied to both.

An important example of instrument differences is the lack of CO_2 slicing channels on VIIRS. The ABI imager on GOES-R [*Heidinger et al.*, 2010] has a very similar channel set to VIIRS (though it also has a single broad, relatively weakly absorbing, CO_2 channel at 13.3 μm). The ABI cloud-top and cloud typing algorithm developed by the GOES-R cloud Algorithm Working Group (AWG) has been ported to VIIRS SDRs (based on the *Heidinger*

et al. [2009; http://cimss.ssec.wisc.edu/patmosx/] PATMOS-x algorithm). In addition, a test version of the MODIS Collection 6 cloud optical/microphysical retrieval code has been ported to VIIRS. Together the merged product replicates similar data sets in the MOD06 file and is referred to in this document as the VIIRS_AWGMOD product. The same common algorithm is capable of running on MODIS L1B data (MODIS_AWGMOD) and will serve as a pathway for bridging the two instrument records. While this is currently being pursued by the team, those results are not shown in this report.

A very simple example of differences due to algorithm choices is that no VIIRS cloud-top parameter or optical property retrievals are generated in the IDPS for pixels classified as probably-cloudy by the VCM. The decision to filter out probably cloudy pixels (not done by the MODIS algorithm) reduces the population of cloud retrievals globally by more than 10%.

The MODIS data record now extends to 13 years for Terra MODIS and nearly 11 years for Aqua MODIS. For the near-term, the VIIRS sensor is the only additional imager that will be available for global cloud retrievals. To ensure the viability of cloud data records that bridge the MODIS/VIIRS time period, alternative approaches to the direct use of the existing IDPS algorithms (or any algorithm out of NASA's control) must be considered. This must be a science-led endeavor, and in particular, the experience and lessons-learned from the MODIS and other heritage sensors need to be brought to bear. The major heritage lesson-learned is that consistent algorithms are needed to continue geophysical data records; continuity of instrument measurement capability is not sufficient.

In summary, it is our strong belief that useful cloud climate records can only be extended across multiple instruments by using the same algorithm approach and assumptions (same forward model assumptions, ancillary sources, pixel filtering, etc.). This is based on the specific results presented in this report as well as our multi-decade experience in cloud retrieval algorithm development and product intercomparisons.

C. Investigating use of CrIS observations to improve cloud top property skill that is lost due to the absence of VIIRS CO_2 slicing channels.

The approach discussed in (B) is the development of a less capable MODIS algorithm that can run on the subset of spectral channels available to both MODIS and VIIRS. This approach to IDPS evaluation and extending/bridging MODIS heritage cloud data records can be thought of as a "lowest common denominator approach" in the sense that a common cloud algorithm is developed for the instrument having the more limited spectral capability (VIIRS in this case). An alternative approach is to try to ameliorate the differences caused by the absence of VIIRS CO_2 slicing channels by using CrIS measurements (and associated spatial resolution issues with CrIS, ~15 km). This has been done using the dual regression approach of *Smith et al.* [2012] and an approach for merging imager and sounder products by *Weisz et al.* [2012]. The dual regression and merged imager/sounder algorithm applied to VIIRS SDRs is referred to in this document as the CrIS_CTP_DS product.

Table 1.1. Overview and comparison of the VIIRS IDPS and MODIS standard cloud products. VIIRS IPs and EDRs are at a spatial resolution of 750 m and 5 km, respectively. All MODIS Level-2 products are available at 1km (at nadir) starting with Collection 6. The notation MODxx is meant to represent both Terra and Aqua MODIS (MYDxx) products.

MODIS Level-2 Product	VIIRS Product	Notes
Detection of Cloudy FOVs		
MODIS Cloud Mask (**MOD35**)	**VIIRS Cloud Mask (VCM)** [ATBD document 474-00033]	IDPS algorithm approach similar to MODIS, though certain spectral tests cannot be implemented with VIIRS due to absence of some water vapor and CO_2 channels.
Cloud Thermodynamic Phase		
part of **MOD06** product separate IR-only (day and night) and solar reflectance + IR algorithms (daytime only)	part of **VCM** derived from brightness temperature tests only	Possibly unique skill with VIIRS 2.25 μm channel (vs. MODIS 2.13 μm), but less capable CTT sanity checks (see below). MODIS C6 IR-based algorithm uses a 7.3 μm water vapor channel not available on VIIRS.
Cloud-Top Properties/Parameters		
part of **MOD06** product cloud-top pressure (CTP) temperature (CTT) height (CTH) starting w/C6 effective emissivity (CEE)	**Cloud Top Parameters (CTP)** [OAD document 474-00083] CTp and CTH. CTT for daytime water clouds. No CEE product.	VIIRS lacks 13.3-14.2 μm CO_2 slicing channels. VIIRS algorithms will inherently have reduced accuracies relative to MODIS for non-opaque high/mid-level clouds. Possible remediation for high clouds with synergistic use of CrIS observations, albeit with coarser spatial resolution.
Cloud Optical and Microphysical Properties		
part of **MOD06** cloud optical thickness (COT) effective particle radius (CER) retrieved separately from 2 SWIR (1.6, 2.13 μm) and 1 MWIR (3.7 μm) channel. Daytime only. liquid and ice water path (LWP, IWP) derived from COT and CER	**Cloud Optical Properties (COP**) [ATBD document 474-00042] CER: uses 1.6 μm channel in daytime and 3.7 μm channel during nighttime. LWP, IWP: not produced. Includes CTT for water clouds at night, and for ice clouds day and night.	CER: VIIRS 2.25 μm channel results in partial lack of microphysical data record continuity w/ MODIS 2.13 μm channel for ice phase clouds (less absorption for VIIRS) due to reduced sensitivity and changes in vertical cloud weighting. The broader and shorter wavelength VIIRS channel in the 1.6 μm window results in more absorption for ice clouds; impact on MODIS data record continuity likely. Both sensors have similar MWIR channels. Quality Assessment (QA): VIIRS lacks 910-940 nm water vapor channels used by MODIS for multilayer cloud detection; uses IR with VIS/SWIR approaches. MODIS land surface spectral albedo from high spatial/temporal resolution gap-filled MODIS land products. VIIRS surface albedo parameterized from surface type. MODIS ice radiative models derived from closure with IR retrievals (C6) using severely roughened aggregated columns. VIIRS ice models based on smooth, multi-habit particles.

We stress that the ported AWG/MODIS algorithms or CrIS algorithms discussed in (B) and (C) are not intended to be a substitute for the NOAA algorithms currently being run in the IDPS. Rather, our algorithm development was intended to be a parallel effort, specifically designed for evaluation and as a pathway for achieving NASA-relevant products for process and climate studies. We note that the JPSS Cloud Cal/Val Team has already produced a report addressing the suitability of IDPS algorithms for operational needs [Heidinger et al., 2012].

1.3 VIIRS IDPS Cloud Products and Mapping to MODIS Heritage Products

An overview of the JPSS IDPS cloud products and MODIS standard products, along with notable differences, is provided in **Table 1.1**. as well as common acronyms for the data set names and individual products used by the production teams. Further details have been provided in Sect 1.1. Note that VIIRS pixel-level Intermediate Product (IPs) are at the M-band 750 m resolution while EDRs are at a scale of 7 km [cf., threshold requirement, JPSS L1RD, Supplement 2.0]. There is no cloud-base product in MODIS as there is little information for that parameter with passive sensors. As such the JPSS cloud base height (CBH) EDR has not been evaluated by our team. CBH is not a standard retrieval parameter for most operational algorithms either. However, the JPSS Cloud Cal/Val team has evaluated CBH using CloudSat observations [*Heidinger et al.*, 2012] and found poor correlations between CBH from the two instruments with the IDPS product having a high altitude bias with respect to CloudSat; interested readers can consult that team's report.

1.4 Overview of Atmosphere PEATE Data Set Production and Tools

The Atmosphere PEATE at the University of Wisconsin-Madison played a key role in this report by enabling the cloud team to have the data sets and analysis tools necessary for the evaluation. In addition to archiving the existing the suite of IDPS product (~1.5 TB/day) and MODIS Collection 5 (C5) datasets, the PEATE processed one year's worth of two team algorithms (see Sect. 1.6): a test version of the MODIS Collection 6 (C6) code and a hybrid code consisting of the NOAA GOES-R Algorithm Working Group (AWG) retrieval algorithm for cloud detection, phase, and cloud-top properties coupled to a MODIS C6-like cloud optical property retrieval code that is applied to VIIRS measurements (referred to as VIIRS_AWGMOD). The PEATE also staged large ancillary datasets for algorithm processing (e.g., high spatial resolution surface spectral albedo data sets used in C6 processing, model analysis, etc.). The PEATE also ingested CALIOP, AIRS, and IASI data.

A critical PEATE tool was the generation of collocated matchup files between the A-Train CALIOP lidar and both MODIS and VIIRS imager pixels (most relevant to Sects. 2 and 3). As mentioned elsewhere, the collocation of CALIOP with VIIRS results in less sampling for the same time period compared with MODIS because the A-Train and NPP orbits synchronize for just a few orbits ever couple of days. Other collocation details are described in later sections. Another important tool developed by the PEATE was a common gridded Level-3 aggregation code that was used to compare global statistics from the four data sets mentioned above. Finally, the entire atmosphere team has worked with the PEATE on a common L1B Intermediate File Format (IFF). While not used in producing team products for this report, the IFF product will be essential as the team moves to implementing a unified hybrid team code on measurements from both VIIRS (VIIRS_AWGMOD) and MODIS (MODIS_AWGMOD).

1.5 Comments on Algorithm Continuity and Trend Detection

The recommendations in this report include algorithm continuity as one element of a strategy for achieving the goal of long-term cloud climate data record continuity into the NPP/JPSS era. By continuity we specifically mean the seamless overlap of cloud retrieval records that allow for climate change detection and analysis. That is, geophysical data records that do not have a significant systematic bias across (or within) the instrument sensors. Detection is known to be an inherently multi-decadal problem for cloud records due to expected small climate change signals embedded within much larger natural variability. This is of course a common challenge for Earth system climate data records.

Here we provide an example of the challenge involved in climate record continuity. Consider trend detection for cloud optical thickness. For context, diagnosis of GCMs indicates that climate feedbacks account for about two-thirds of equilibrium climate sensitivity, with cloud feedback constituting the largest source of inter-model uncertainty (e.g., a $2xCO_2$ climate sensitivity standard deviation of about 0.5K in the *Dufresne and Bony* [2008] study). A number of studies have shown that changes in low marine clouds in the (sub)tropics are the largest cause of the inter-model spread in the global net cloud feedback [*Bony and Dufresne*, 2005; *Webb et al.*, 2013; *Zelinka et al.*, 2012a,b]. As such, detection of basic cloud property trends (fraction, height, optical thickness) associated with a warming climate are a fundamental observation, and are listed as an Essential Climate Variables (ECVs) by the international Global Climate Observing System (GCOS).

Regarding the climate signal, zonal and/or regional trends in cloud optical thickness are typically less than 5%/decade for a set of five CMIP5 models simulating an abrupt quadrupling of CO_2 analyzed in a recent study [*Zelinka et al.*, 2013 and private communication]. As shown in **Fig. 1.1**, zonal means are in excess of 5%/decade only in polar regions; much lower means in the (sub)tropics are often associated with regional trends that can exceed a few percent per decade but vary in sign as a function of longitude (not

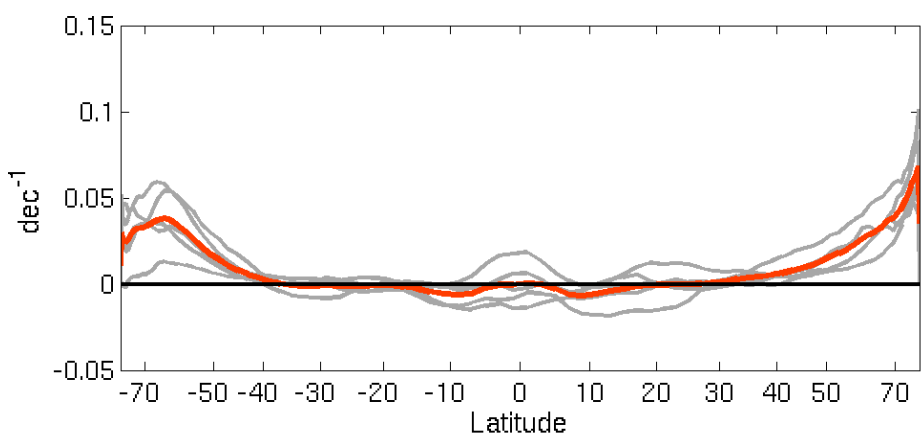

Fig. 1.1. Zonal mean decadal trend in cloud optical thickness (relative change/decade) derived from simulator output for 5 CMIP5 models [*Zelinka et al.*, 2013; private communication]. Individual models are given by the gray lines; the inter-model mean is given by the red line.

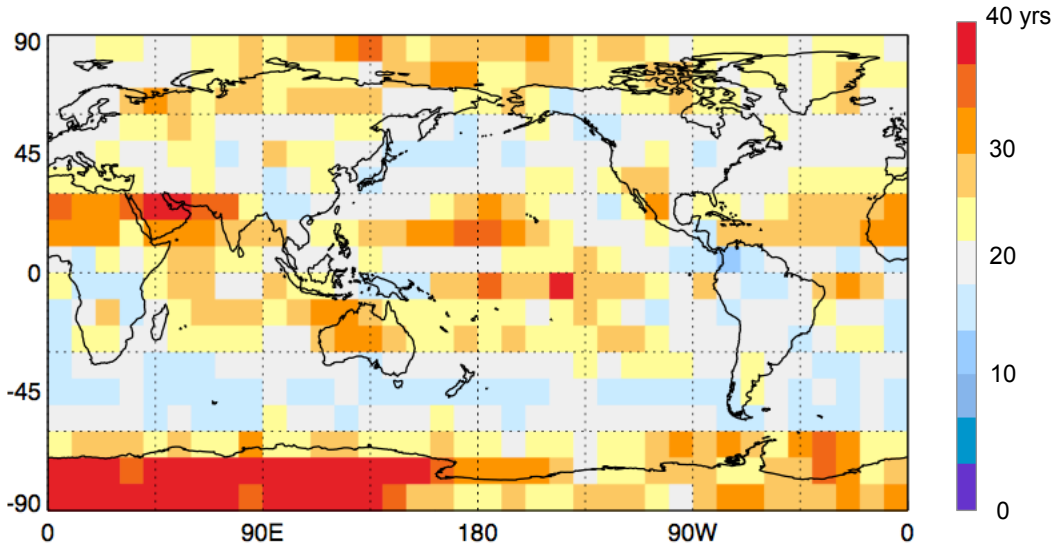

Fig. 1.2. Time required to have a 90% probability of detecting a trend to a statistical significance of 0.05 if a 5%/decade change in cloud optical thickness was occurring in each 10° grid box. Variability and correlation statistics needed for deriving time-to-detection are from 12 years of MOD06 C5 cloud data.

shown). The figure shows the relative change in the cloud fraction-weighted optical thickness using model ISCCP simulator output [*Zelinka et al.*, 2012a] where feedback (cloud parameter change per surface ΔT_s) has been mapped to a time scale using each model's individual warming trends.

The time required for trend detection of cloud optical thickness (combined phases) is shown in **Fig. 1.2**, derived from 12 years of MODMOD06 Terra retrievals and assuming that the actual trend in each 10° grid box is 5%/decade [from *Platnick et al.,* 2011 presentation, based on *Tiao et al.*, 1990 and *Weatherhead et al.*, 1998]. The time-to-detection is 15-20 years at a minimum and often exceeds a few decades in the (sub)tropics and polar regions. That is, even under ideal circumstances (perfectly stable instrument radiometry and a consistent algorithm) the existing MODIS record is not yet long enough to detect trends to the 5% level at this grid resolution. Smaller trends will of course take longer to detect. Detection of a 2% trend takes almost twice as long as for a 5% trend (time-to-detection scales to the ⅔ power). As another anchor point, the observational stability requirements for cloud optical thickness climate data records was given as 2%/decade (with 10% accuracy) by *Ohring et al.* [2005] though the spatial aggregation scale was not specified. Interannual climate variability (e.g., ENSO) can also increase the detection time.

The impact of introducing a fixed unknown systematic offset into a data record at a known time (e.g., appending the IDPS VIIRS cloud data record to the MODIS record at some point) can be modeled. The impact on trend significance and trend detection depends on where in the record the offset is introduced as well as natural variability, but not directly on the expected value of the offset that comes out of the least squares regression. As expected, the impact is lessened if one or the other of the two records makes up a small fraction of the overall time record. An approximation for the factor increase in the standard deviation (uncertainty) of the calculated trend is $f=[1-3\tau(1-\tau)]]^{-1/2}$, where τ is the fraction of

the time record coming from the initial data set [*Weatherhead et al.*, 1998]. The maximum value of f is 2 when both data sets are equal contributors (τ=0.5), and the confidence level in the trend decreases substantially. Similarly, the time-to-detection (using same statistical significance as in **Fig. 1.2**) increases by roughly $f^{2/3}$ or about 1.6 for τ=0.5 [*Weatherhead et al.*]. For example, consider a MODIS record that is discontinued after 12.5 years (e.g., late 2014 for Aqua) and replaced by an IDPS record. A grid box in Fig. 1.2 for which a 5% trend would have taken 25 years for MODIS to detect (yellow color) will now require about a 40 year detection time. The much more realistic situation where the retrieval offset is not constant but has a time dependence (e.g., seasonal) and/or depends on the cloud parameters which are changing on decadal scales, will be much more problematic - if not impractical to model. Note that once an offset is included as part of the statistical model, the uncertainty in the null hypothesis (offset equal to zero) is always non-zero, that is, a perfect match between the two data sets cannot be established with absolute certainty. This is the reason that the trend and time-to-detection increase regardless of the expected value of the offset.

The above impacts occur when the offset is part of the statistical model. However, even worse would be the situation where the offset is ignored in the trend calculation. Neglecting autocorrelation, the bias in the trend is estimated as $60\delta\tau(1-\tau)/n$, where δ is the systematic offset introduced into the record, the trend is in units of per decade, and n is the length of the record in years [*Weatherhead et al.*, 1998]. Continuing with the previous example, τ=0.5 and n=25 yrs gives a trend bias of 0.6δ, e.g., a systematic offset of 3% would result in a trend bias of roughly 2% [stability metric from *Ohring et al.*, 2005] for that time period if the offset is not accounted for.

The message here is that any systematic offset in the optical thickness data record of order several percent relative due to algorithm inconsistency may be expected to significantly alias into the climate signal and decrease the trend confidence and the time-to-detection of the actual signal. Or worst yet, result in a significant bias in the trend calculation if the offset is not modeled. Further, it seems unlikely that that an offset in an IDPS vs. MODIS record would be fixed in space/time and therefore be impractical to model. Similar statements can be made for cloud fraction (cloud masking) and cloud top pressure. Sections 2–4 show a number of examples of systematic differences between IDPS and heritage cloud products being far in excess of several percent relative. A summary of systematic monthly mean differences for each month inclusive of March 2012 through January 2013 are summarized in the figures of Sect. 1.6.

Reducing systematic cloud product biases across the MODIS and VIIRS instruments is inherently challenging because of important instrument channel differences described below. To reduce the large systematic biases found in this report, it is our experience that common pixel-level geophysical algorithms applied to both the MODIS and VIIRS sensors are required to the extent possible.

Continuity requirements for short-term or instantaneous studies (process studies, model assimilation, applications) may be different. That said, most VIIRS IDPS cloud products analyzed in this report still fall short relative to MODIS for short-term studies due to the absence of key absorption spectral channels (see Sects. 3 and 4 in particular). However, whether for climate or shorter-term uses, the report provides a path forward to help reduce the absence of missing channels through the inclusion of CrIS measurements.

Input from the presentation of this strategy at science team meetings suggests that these recommendations can be misunderstood or taken out of context. We stress that the common algorithm approach recommended for establishing a multi-decadal MODIS/VIIRS climate record does not mean that NASA should not move forward to obtain improved instrument measurement capabilities and derived physical records in order to better understand processes that define the climate system and perhaps begin a new generation of improved climate data records; climate record continuity and instrument/retrieval advancements are complementary endeavors. Furthermore, a common algorithm does not mean that ESD should abandon support to refine and maintain cloud products for the most spectrally capable instrument (MODIS) as long as sensor performance allows.

1.6 Annual Cycle of IDPS IP Cloud Products

Examples of aggregated tropical/midlatitude monthly mean IDPS IP cloud products relative to heritage (MODIS C5 and/or C6) and the VIIRS_AWGMOD team algorithm are shown in **Fig. 1.3** for an 11-month period beginning in March 2012. The C5 data were acquired from the MODIS distribution site (LAADS); the C6 and AWGMOD algorithms were processed at the PEATE. A common aggregation code was applied to each data set using the same assumption. For example, to be consistent with the MOD08 Level-3 algorithm, these aggregations use pixels from multiple (overlapping) swaths in populating the grid boxes. Aggregations are for the daytime only. A comparison of C5 means against the standard MOD08 product were found to be equivalent to much better than a fraction of a percent relative. However, we do note that the VIIRS SDR file deletes so-called "bow tie" pixels, whereas these pixels are included in MODIS Level-2 and Level-3 processing.

For context, the grey boxes to the right of each row shows the magnitude of a signal that is equivalent to 5% of the MODIS C6 mean. *With the exception of cloud fraction (from the cloud mask products) and liquid water effective radius after August 2012, the differences between IP (black curves) and heritage products (green) are significant with respect to the discussion of Sect. 1.5*. Based on the information at hand, the cause of the August change in liquid water effective radius is unknown. Further, the AWGMOD team algorithm run on VIIRS measurements (red curve) is generally much closer to heritage means than the IP product, and this is before a MODIS-like (or VCM-like) cloud mask has been incorporated.

The ice cloud optical thickness plots (second row) show dramatic differences between MODIS C5 and C6 means. The decrease in C6 means is due to a new ice model LUT (comprised of only severely roughened aggregated columns) that provides spectral closure with IR observations; *this particular example clearly emphasizes our point that algorithm consistency, including radiative transfer forward models, are essential to data record continuity*.

We note that in some instances a histogram of retrievals is required to provides meaningful context to algorithm differences. This is true in particular for CTP where mean values can be ambiguous. For example, algorithms can provide the same mean value in grid box even though the fraction of high and low clouds might be dramatically different. This is the case in the IP comparisons of **Fig. 1.3**. As shown later on in Sect. 3 (e.g., Fig. 3.3), the IP

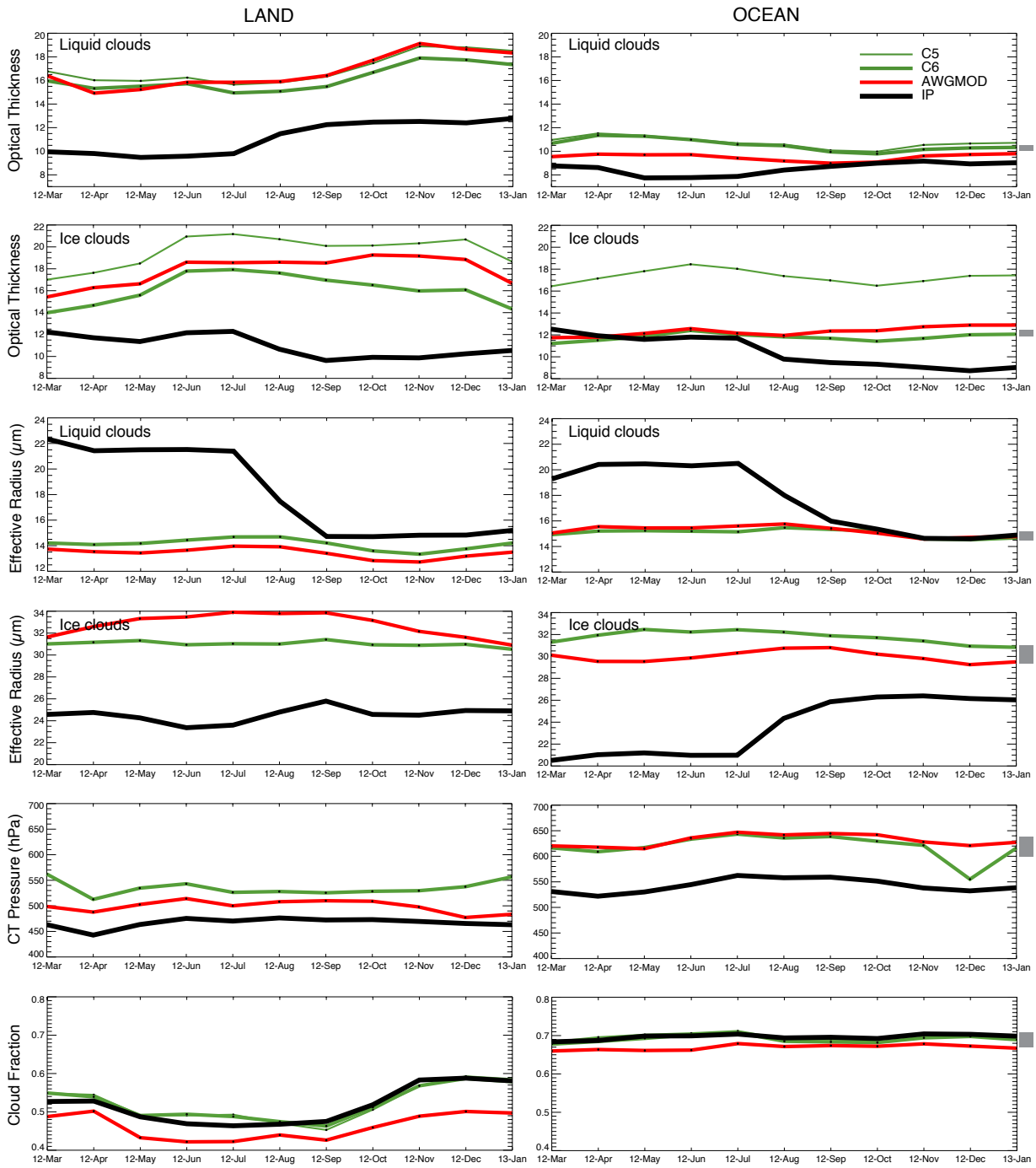

Fig. 1.3. Near-annual cycle in mean cloud properties over land and ocean averaged over ±60° latitude for the following four datasets: VIIRS IDPS pixel-level Intermediate Product (IP), MODIS C5 (except CTP where the dataset was not available at the 1km pixel scale), MODIS C6 science test code where all products are at the 1km pixel scale, and the hybrid VIIRS_AWGMOD team product at the IP pixel scale. For context, the grey shaded boxes to the right of each row shows the magnitude of a signal that is 5% of the MODIS C6 mean. With the exception of cloud fraction and liquid water effective radius after August 2012, there are significant differences between the IP and other data sets.

cloud-top heights show different biases with respect to MODIS depending on the altitude of the cloud-top; the IP product has a high-altitude bias for low clouds and a low-altitude bias for high clouds). Depending on the fraction of high and low clouds over the ±60° domain of Fig. 1.3, the means can be quite close but for the wrong reasons. Radiatively, obtaining a correct mean pressure but incorrect histogram (biases that are a function of cloud height) will give an incorrect LWIR TOA flux.

2. VIIRS Cloud Mask and Thermodynamic Phase (VCM)

2.1 Comparison of Key Algorithm Approaches: IDPS vs. MODIS

The VCM is modelled after the MODIS cloud mask [*Hutchison et al.,*2005; *Hutchison and Cracknell*, 2005; and *Hutchison et al.,* 2008]. As with the MODIS cloud mask [*Ackerman et al.*, 1998, *Frey et al.*, 2008, *Baum et al.*, 2012], the output of the VCM algorithm is 6 bytes (48 bits) for each moderate resolution pixel. The mask includes information about the processing path the algorithm took (e.g., land or ocean) and whether a view of the surface is obstructed. After the cloud confidence is determined, the VCM tests the pixel for aerosols and fires. Algorithms to generate the VIIRS cloud, aerosol, land, ocean, surface temperature, and snow/ice Environmental Data Records (EDRs) use the VCM as auxiliary data as mandated by the VIIRS Interface Data Processing Segment (IDPS).

Cloud mask algorithms for both VIIRS and MODIS use a series of spectral tests on the radiances or their associated brightness temperatures. Cloud detection is based on the contrast (i.e., cloud versus background surface) in a given target area—in this case, at the pixel resolution. Contrast may be defined as differing signals for individual spectral bands (e.g., clouds are generally more reflective in the visible but colder than the background as measured in the thermal IR), spectral combinations (e.g., 0.86/0.66 μm ratio is close to unity for cloudy skies), or temporal and spatial variations of these. Both the VIIRS and MODIS cloud masks use several cloud detection tests to indicate a level of confidence that the observation is a clear-sky scene. The cloud mask is produced for the entire globe, day and night.

Both cloud masks assess the likelihood that clouds obstruct a given pixel. As cloud cover can occupy a pixel to varying extents, the cloud mask is designed to allow for varying degrees of clear-sky confidence (i.e., it provides more information than a simple yes/no decision).

The VCM cloud phase uses IR and solar reflectance channels during daytime observations, but of course only uses IR channels at night. Therefore, there is a discontinuity in phase information content between daytime and nighttime observations.

2.2 Evaluation Methodologies

IDPS VCM results were evaluated against the: (1) Collection 5 or 6 Aqua MODIS cloud mask (MYD35); (2) PATMOS-x cloud mask algorithm [*Heidinger et al.,* 2009, http://cimss.ssec.wisc.edu/patmosx/] which has historic value for satellite climate studies; (3) CALIOP lidar cloud detection from the CALIPSO satellite. Because of the similarity of the VCM and MODIS cloud algorithms, both masking results are compared to collocated CALIOP observations.

The first two bits of the mask summarize the results from all individual tests by classifying every pixel of data as either confident clear, probably clear, uncertain/ probably cloudy, or cloudy. To be classified as clear in this analysis, all VIIRS and MODIS pixels within a group were required to be labeled as confidently clear or probably clear. Those labeled as probably cloudy or cloudy are considered cloud contaminated scenes.

IDPS thermodynamic phase retrievals (IP scale) were evaluated against collocated CALIOP cloud-top phase retrievals (1 km scale collocations) and hit rates determined using CALIOP as truth. Collection 5 Aqua MODIS IR phase retrievals (MYD06) that are at a 5 km scale are also compared against collocated CALIOP phase retrievals in a similar manner (though with 5 km scale collocations) to provide a base comparison to help interpret the VIIRS comparison. Direct comparison of MODIS with VIIRS can be ambiguous as discussed below, so a geographic comparison of the number of pixels in categories ice and water over the same time period is conducted to assist in the assessment of algorithm differences.

Assessment of the VCM cloud phase product as a climate data record is not as straight forward as one might expect. The water phase included in the VCM is first assessed through comparisons with the collocated [*Holz et. al.,* 2008] CALIOP water phase product. There are no VIIRS phase retrievals for cloud mask conditions of probably clear or probably cloudy. In addition, in this comparison we included the VIIRS "Water Cloud", "Opaque Ice Cloud" and "Cirrus" categories, and did not include "probably water", "Supercooled Water/ Mixed Phase" and "Cloud Overlap". Inclusion of these ignored categories would likely yield less agreement and make interpretation more confusing. Further, the higher resolution 1 km scale CALIOP collocations used in the VCM phase comparisons are likely to have less cirrus detection than the 5 km scale collocations used in the MODIS IR comparisons due to less spatial averaging. This may cause sampling differences between the two collocations. Finally, as already mentioned, the VCM uses a different phase algorithm for daytime observations.

There are significant differences between MODIS IR and VIIRS IR/solar cloud phase products. MODIS retrieves a phase if there are at least 4 cloudy plus probably cloudy pixels in a 5x5 group of pixels. MODIS has no cloud overlap category while VCM phase has no uncertain category. VIIRS uses no "probably cloudy" pixels in its phase retrieval algorithm. We do not attempt to make comparisons with the IR/reflectance based C5 MYD06 retrieval phase (1 km) because it is only available for successful COP retrievals, making the comparisons more ambiguous.

2.3 Evaluation Results

Figure 2.1 shows the global distribution of cloud amount derived from VCM and PATMOS-x using the VIIRS observations [Heidinger et al., 201] for 29 November 2012 in the ascending node of the spacecraft. As expected, the large-scale patterns are similar to other satellite data sets of cloud amount [Rossow et al., 1993; Thomas et al., 2004; Wylie et al., 1994; *Maddux et al.,* 2011, *King et al.,* 2013, *Stubenrauch et al.,* 2013]. The Intertropical convergence zone (ITCZ) is clearly evident as are the subtropical high-pressure systems and the marine stratocumulus regions. **Figure 2.2** shows the global map of the difference between the two analysis methods. White regions indicate both VCM and PATMOS-x detect cloud, while green and blue regions are where both methods detect clear over land and water, respectively. Regions colored cyan indicate where the VCM de-

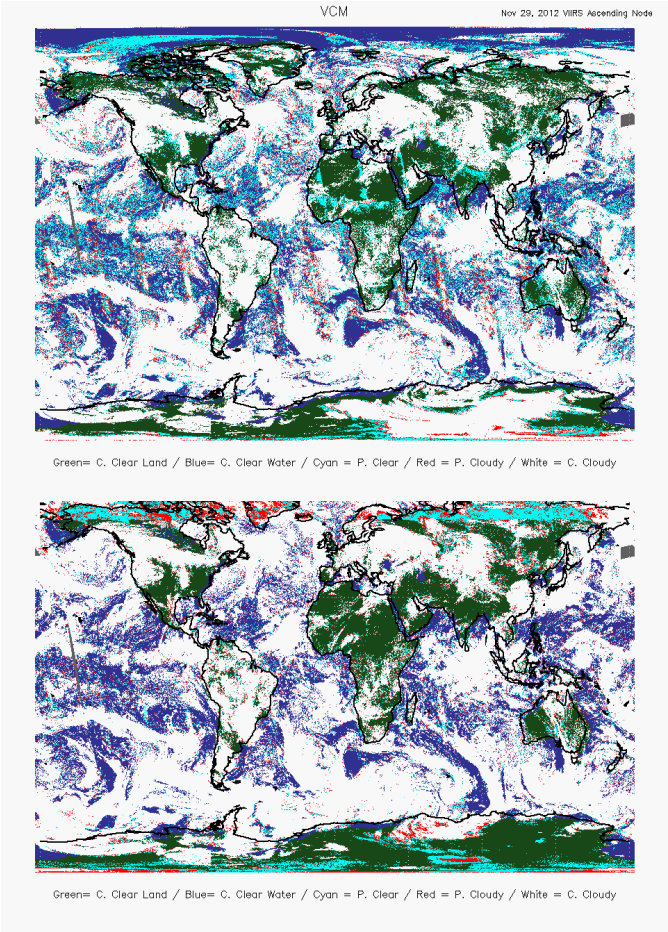

Fig. 2.1. Results from VCM (top) and PATMOS-x (bottom) cloud mask algorithms applied to VIIRS for data collected in ascending orbit, 29 Nov. 2012.

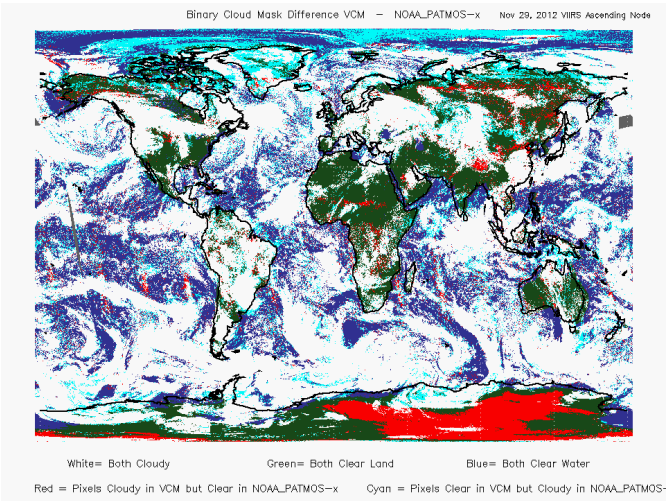

Fig. 2.2. Difference between VCM and PATMOS-x cloud mask algorithms applied to VIIRS data collected in ascending orbit, 29 Nov.2012. Green and blue regions are where both methods detect clear over land and water, respectively. Cyan regions indicate where the VCM detected clear while the PATMOS-x detected cloud; red pixels are where the VCM assigned cloudy and PATMOS-x clear.

tected clear while the PATMOS-x detected cloud; red pixels are where the VCM assigned cloudy and PATMOS-x clear. The two algorithms are applied to the same input data (VIIRS SDRs), so differences in the performance arise from the differences between the algorithms. There is generally good agreement between about 60S and 60N, with the VCM producing more clouds in the southern polar region, and less cloud to the north of 60N.

In the next analysis, we compare VCM and PATMOS-x cloud detection results using VIIRS input observations, and also PATMOS-x and Collection 6 MODIS cloud mask (MYD35) results using input MODIS observations for data collocated during the time period 10 November 2012 to 29 November 2012. Only data within ±0.2 hours (±12 minutes) of the collocation window between satellites is used in the comparison (a filter on cloud optical thickness was not applied). In the first comparison we focus on scenes where, in general, cloud masks perform the best – ocean only regions between 60N – 60S during the daytime with no surface ice. The results are shown in **Table 2.1** where the first column is the algorithm, the second is the sample size, column 3 is the cloud fraction detected by CALIOP lidar, column 4 is the cloud fraction from each algorithm listed in column 1, 5-6 provide the percent of probably clear and probably cloudy pixels, and the final three columns are more comparisons with CALIOP. Leakage refers to missed clouds, where the lidar is cloudy and others confidently/probably clear. While improvements could be made to the VCM, overall it performs well, detecting 93% of the clouds detected by CALIOP, with false detections and leakages of 1.6% and 5.2% respectively. The differences between the two PATMOS-x results indicate that the VIIRS performance suffers from lack of water vapor bands that are available on MODIS.

Polar regions are much more difficult environments in which to discriminate between clear and cloudy pixels, as shown in **Table 2.2** where we summarize results for all scenes poleward of 60N. These results demonstrate needed improvements for the VCM.

We next compare zonal mean cloud frequencies between the VCM and CALIOP lidar during the 33-day period 20 September to 22 October 2012. Collocation was conducted and described by *Holz et al.* [2008]. **Fig. 2.3** (top) shows the results as a function of day and night. While the VIIRS and CALIOP instruments have very different scanning methods, *Ackerman et al.* [2008] demonstrated that zonal means can be well represented by both broad swath scanning and near-nadir viewing instruments. In general, the VCM has a lower zonal cloud frequency during both daytime and nighttime. These differences can be particularly large in polar regions where differences can exceed 20%. For reference, we show the same comparison (bottom) but use the C6 MODIS cloud mask. Outside the polar regions, there is excellent agreement. Maximum differences occurring during polar night, consistent with results of *Ackerman et al.* [2008] and *Holz et al.* [2008].

A global comparison of the CALIOP, VCM, and MODIS cloud mask results for the same 33 day period is presented in **Tables 2.3 and 2.4**. For the comparison, a VCM or MODIS cloud mask result is considered cloudy if the cloud mask returns confident cloud or probably cloudy, while a pixel is defined clear if the cloud mask returns probably clear or confidently clear. Only pixels where all the collocated CALIOP retrievals are identical (i.e. either all clear or all cloudy) are included in the statistics in **Tables 2.3 and 2.4**.

Table 2.3 shows hit rates (in comparisons to CALIOP) for MODIS Collection 6 MYD35 and VCM for CALIOP cloud optical thicknesses greater than 0.3, while **Table 2.4** shows comparisons for all optical thicknesses. Column 1 in each table lists the scene category,

and columns 2-3 show the hit rate for the Collection 6 MOD35 and VCM masks. The hit rate is defined as $100(N_{cld} + N_{clr})/N$ where N_{cld} is the number of cloud pixels in agreement, N_{clr} is the number of clear pixels in agreement, and N is the total number of collocated pixels. The agreement is also expressed by the Hanssen-Kuipers Skill Score [*Hanssen and Kuipers*, 1965]. The score has a range of -1 to +1, with 0 representing no skill. This skill score expresses the hit rate relative to the false alarm rate, and will remain positive as long

Table 2.1. Cloud mask results and comparisons for VCM and PATMOS-x algorithms using VIIRS observations, and also PATMOS-x and C6 MOD35 algorithms using input MODIS observations data collocated during the time period 10–29 November 2012 for ocean only regions between 60N–60S during the daytime with no surface ice. The first column is the specific algorithm, the second column the sample size, column 3 is cloud fraction from CALIOP lidar, 4 is the same for each algorithm in column 1, 5-6 provide the percent of probably clear and probably cloudy, and the final three columns show more comparisons with CALIPSO. Leakage refers to the cases of missed clouds where CALIPSO is cloudy and the others confidently/probably clear.

Cloud Mask Algorithm	**Sample Size**	**Cloud fraction**				**Probability of**		
		Active	Passive	Pr. Clear	Pr. Cloudy	Correct Detection	False Detection	Leakage
VCM	154160	0.773	0.737	0.062	0.025	0.932	0.016	0.052
NOAA PATMOS-x VIIRS	154160	0.773	0.762	0.009	0.009	0.950	0.020	0.029
NOAA PATMOS-x MODIS	106461	0.781	0.773	0.009	0.010	0.977	0.008	0.015
MODIS_C6	106461	0.781	0.776	0.029	0.016	0.973	0.011	0.016

Table 2.2. Same as Table 2 except for all scenes poleward of 60N.

Cloud Mask Algorithm	**Sample Size**	**Cloud fraction**				**Probability of**		
		Active	Passive	Pr. Clear	Pr. Cloudy	Correct Detection	False Detection	Leakage
VCM	23941	0.769	0.412	0.137	0.048	0.613	0.015	0.372
NOAA PATMOS-x VIIRS	23941	0.769	0.714	0.246	0.204	0.803	0.071	0.126
NOAA PATMOS-x MODIS	38637	0.724	0.610	0.246	0.165	0.813	0.036	0.151
MODIS_C6	38637	0.724	0.650	0.016	0.077	0.839	0.044	0.118

as the hit rate is greater than the false alarm rate; it is a useful metric when analyzing phenomena that are not normally distributed. Columns 4-5 of **Table 2.4** give the Hanssen-Kuipers Skill Score for MOD35 and VCM respectively.

The global and regional agreement between MODIS and CALIOP is generally greater than 88%, while VCM hit rate for all cloud optical depths is generally less than the hit rate of MODIS by more than 5%. Agreement between the hit rates of MODIS and VCM improves when comparison is categorized to COT > 0.3, indicating that VCM is missing some optically thin clouds. The skill score of the VCM is always less than the MODIS (**Table 2.4**). As expected, both cloud masks have their highest hit rates for daytime ocean scenes between latitude belts of ±60°, although the skill score of the VCM is still 10 points below the MODIS algorithm.

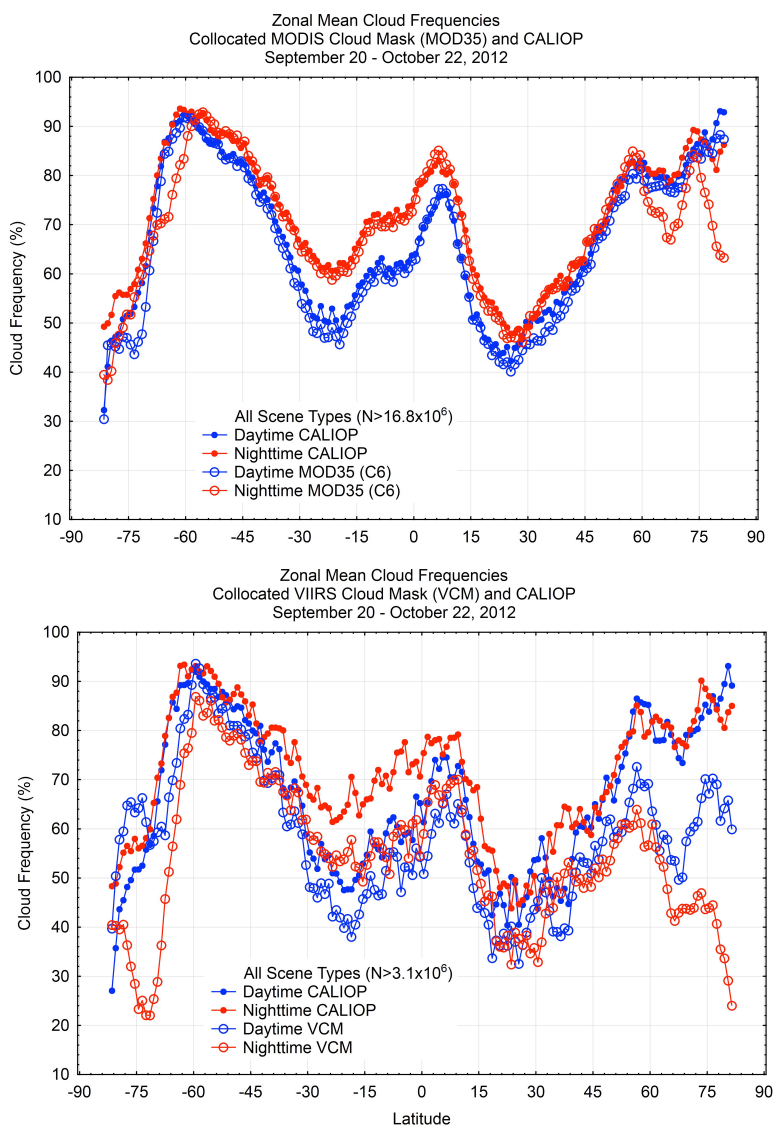

Fig. 2.3. Zonal mean cloud frequency for CALIOP and VCM (top) for the period September 20 through October 22, 2012. The bottom figure shows the same comparison for CALIOP and MODIS MOD35 Collection 6 algorithm.

The assessment of polar regions is summarized in **Tables 2.5 and 2.6** where the MODIS cloud mask (MYD35) and VIIRS cloud mask (VCM) are compared to the collocated polar CALIOP cloud detection product for 20 September to 22 October 2012. The comparisons are also broken out for Greenland and Antarctica. There is significant improve-

Table 2.3. MODIS MYD35 and VCM hit rates (in comparison to CALIOP) for CALIOP cloud optical thicknesses greater than 0.3. Column 1 lists the scene category, and columns 2-3 show the hit rate for the Collection 6 MOYD35 and VCM masks.

Scene Category	MYD35 C6 Hit Rate	VCM Hit Rate
Global	90.7	81.4
60S-60N	93.7	90.9
Global Day	92.5	85.4
60S-60N Day	94.5	91.2
Global NIght	89.1	77.9
60S-60N Night	92.9	90.7
60S-60N Water Day	94.8	91.6
60S-60N Water Night	93.3	91.5
60S-60N Land Day	93.8	89.9
60S-60N Land Night	92.0	88.9
Desert Day	93.6	92.5
Desert Night	93.2	93.1

Table 2.4. MODIS MYD35 and VCM hit rates (in comparisons to CALIOP) for all cloud optical thicknesses. Column 1 lists the scene category, and columns 2-3 show the hit rate for the Collection 6 MYD35 and VCM masks. Columns 4-5 show the Hanssen-Kuipers Skill Score for MYD35 and VCM respectively.

Scene Category	MYD35 C6 Hit Rate	VCM Hit Rate	MYD35 Hanssen-Kuipers SS (%)	VCM Hanssen-Kuipers SS (%)
Global	88.0	76.0	74.7	57.4
60S-60N	90.9	83.7	80.0	70.6
Global Day	89.8	80.7	78.6	62.2
60S-60N Day	91.3	84.7	82.0	71.1
Global NIght	86.4	72.0	71.1	53.3
60S-60N Night	90.5	82.8	77.5	70.4
60S-60N Water Day	92.1	85.6	81.9	71.1
60S-60N Water Night	91.0	83.2	76.0	69.4
60S-60N Land Day	89.1	82.0	78.8	65.6
60S-60N Land Night	89.3	81.7	78.3	67.3
Desert Day	88.4	87.9	69.4	56.7
Desert Night	89.1	87.4	76.1	56.5

Table 2.5. MODIS MYD35 and VCM comparison to collocated CALIOP observations for all cloud optical thicknesses. Scene category is followed by the total matchups, hit rate and Hanssen-Kuipers Skill Score for MODIS Collection 6 and VCM, respectively.

Scene Category	C6 MYD35			VCM		
	Total MYD35 Matchups	Overall Hit Rate (%)	Hanssen-Kuipers SS (%)	Total VCM matchups	Overall Hit Rate (%)	Hanssen-Kuipers SS (%)
Polar	5598489	82.1	63.7	1174690	63.2	33.9
Polar Day	2250029	86.2	68.8	487437	72.9	42.4
Polar Night	3348460	79.4	60.4	687253	56.3	28.8
Arctic Day	1048920	90.8	72.5	216309	75.0	60.5
Arctic Night	1751063	81.1	63.3	381092	54.7	41.3
Antarctic Day	1201109	82.2	63.8	271128	71.2	36.9
Antarctic Night	1597397	77.6	56.9	306161	58.3	22.9
Greenland Day	83106	78.3	57.2	17103	62.2	34.4
Greenland Night	174130	73.5	51.2	34837	47.3	15.0
Antarctica Day	517587	67.4	30.5	129403	58.3	20.5
Antarctica Night	833811	75.2	50.1	196390	54.1	8.0

Table 2.6. VCM comparisons to CALIOP for all cloud optical thicknesses and optical thicknesses greater than 0.3. Column 1 lists the scene category, followed by the total matchups, hit rate and Hanssen-Kuipers Skill Score for VCM in polar regions for data collected from September 20 to October 22, 2012.

Scene Category	All CALIOP COT			Clouds with CALIOP COT>0.3		
	Total VCM Matchups	Overall Hit Rate (%)	Hanssen-Kuipers SS (%)	Total VCM matchups	Overall Hit Rate (%)	Hanssen-Kuipers SS (%)
Polar	1174690	63.2	33.9	1002796	67.2	38.6
Polar Day	487437	72.9	42.4	419673	75.2	46.4
Polar Night	687253	56.3	28.8	583123	61.4	33.9
Arctic Day	216309	75.0	60.5	177473	78.5	64.1
Arctic Night	381092	54.7	41.3	316799	60.4	46.4
Antarctic Day	271128	71.2	36.9	242200	72.7	41.0
Antarctic Night	306161	58.3	22.9	266324	62.6	28.1
Greenland Day	17103	62.2	34.4	15549	66.2	38.6
Greenland Night	34837	47.3	15.0	30626	52.3	18.7
Antarctica Day	129403	58.3	20.5	117731	58.6	25.2
Antarctica Night	196390	54.1	8.0	171761	58.2	12.4

Table 2.7. Global agreement between VCM, C5 MODIS IR, and CALIOP cloud phase products as a function of CALIOP phase for day and night retrievals combined. Collocations are for September 20 to October 22, 2012. Entries are in percent; the total sum in each column is 100. Imager entries corresponding to CALIOP phase are boldfaced.

VCM Phase	CALIOP Phase		
	Liquid (water and possibly water categories)	Ice (including mostly or possibly randomly orientated, and possibly horizontal oriented ice particles)	Unknown Phase
Water	**36.1**	9.9	13.0
Opaque Ice	0.2	**7.2**	1.0
Cirrus	3.8	**30.4**	9.0
Mixed	51.8	21.1	**65.0**
Overlap phase layers	8.0	31.4	**12.0**

MODIS C5 IR Phase	CALIOP Phase		
	Liquid (water and possibly water categories)	Ice (including mostly or possibly randomly orientated, and possibly horizontal oriented ice particles)	Unknown Phase
Water	**54.8**	9.9	25.5
Ice	4.9	**56.1**	7.8
Mixed	7.0	14.8	**17.6**
Undecided	33.3	19.1	**49.0**

ment needed for the VCM under these challenging conditions.

To evaluate the VCM phase results, **Table 2.7** shows the percent agreement between the VCM and MODIS C5 IR product for scenes that CALIOP identifies as liquid water, ice (with various orientations), or unknown phase. The best agreement is for MODIS with between 55%–67% agreement for the three CALIOP phase categories (both MODIS mixed and undecided categories considered in agreement with the CALIOP unknown phase). In contrast, the VCM phase is in agreement with the liquid and ice phase only 36% and 38% of the time, respectively, with 78% agreement for unknown phase (mixed and overlap). As already mentioned, these comparisons can be misleading as they are not using the same pixel population. Another comparison to conduct is to analyze the number of pixels identified as water or ice by MYD06 and VCM for the same time period. This is shown in **Fig. 2.4**, demonstrating that indeed a different population of pixels are labeled as water or ice

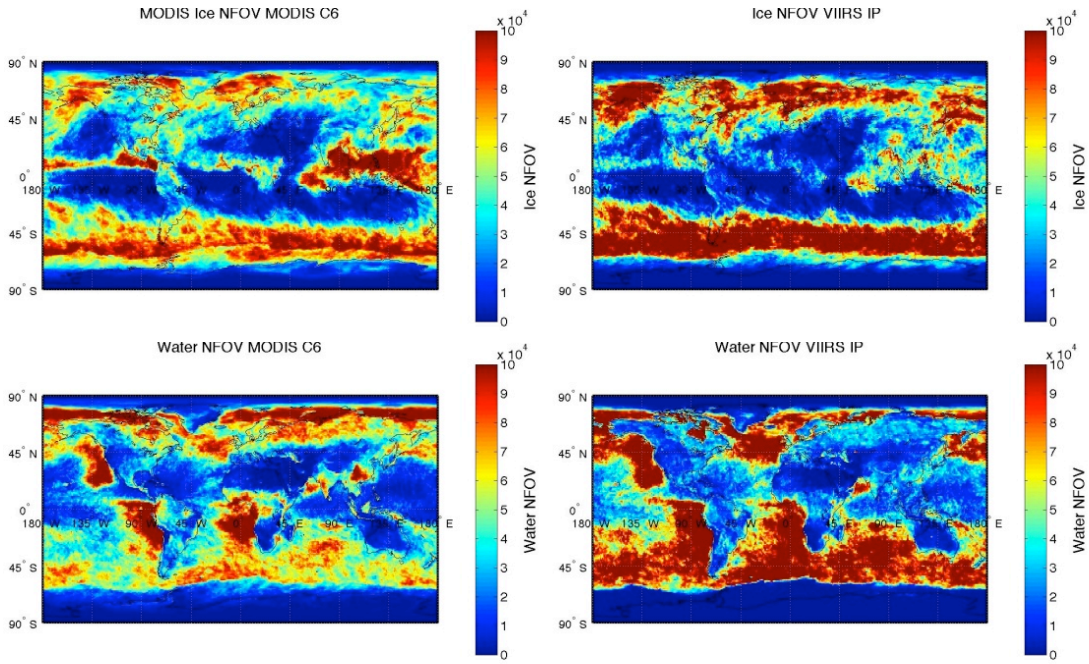

Fig. 2.4. The number of fields-of-views (pixels) categorized as ice or water (top and bottom figures) for MODIS and VCM (left and right figures).

by the two algorithms. The large discrepancies demonstrate the lack of algorithm continuity needed for cloud climate records to bridge the different instruments.

2.4 Conclusions

The VCM assessed in this report is the algorithm that was implemented into the IDPS processing in late April, 2012. While it does not meet MODIS capabilities, algorithm changes can likely be made to improve the VCM results. For example, ancillary snow maps used by the VCM should not be static. The problem is that making changes in the IDPS is both time consuming and tedious. Thus, reprocessing the VIIRS data for climate data records is a challenge in the IDPS.

While there are important performance concerns with the VCM as described in the previous section, a major issue with using the VCM for climate studies reside with the IDPS processing system used in the JPSS Ground Segment. Our issues with the IDPS for climate studies are listed below.

- The IDPS has not been stable during the first year of NPP operation and shows signs of continued instability. For example, the VCM relies on knowledge of the surface to select appropriate cloud detection thresholds. The IDPS functions that provide information on snow and vegetation cover remain non-functional. Issues also remain with the interaction of the VCM with these background fields. These changes cause large impacts in the VCM performance and will certainly destroy the stability needed for climate data records. Presumably this will eventually be solved but their continued presence one year after launch and many years after development is troubling.

- It is clear that the IDPS systems located at the central processing sites are not designed for reprocessing. Our experience is that climate quality data is never generated until multiple passes through the data are accomplished. Our limited experience with the IDPS indicates that it does not provide an avenue for the reprocessing that we believe is required.
- ADL software is provided as the mechanism for the community to process IDPS algorithms outside of the IDPS. We have found ADL to be slow and cumbersome to use. Tools to acquire the ancillary data for running ADL are lacking and for this reason, large scale processing with ADL is impossible. We do not see ADL as an option for NASA climate needs.

Given the reasons above, one could still use the VCM outside of the IDPS or ADL. This option has been explored. However, IDPS algorithms are in general written specifically for the IDPS interfaces. Emulating these interfaces has been very difficult and time consuming. To date, the PEATE has still not achieved the ability to match the IDPS VCM with enough accuracy to consider exploring using the VCM outside of the IDPS for climate work.

3. Cloud Top Parameters (CTP)

Cloud Top Parameters refer to cloud-top height, cloud-top temperature and cloud-top pressure environmental data records (EDRs). The goal of this section is determine the viability of the IDPS VIIRS EDRs to continue EOS NASA and other heritage data records. CTPs are important for climate research since they provide information on the vertical distribution of cloudiness and the impact of clouds on the radiation budget. In addition, cloud height assimilation is of growing importance in NWP data assimilation and cloud height climatologies will likely play a role in future NWP Reanalysis efforts.

3.1 Comparison of Key Algorithm Approaches

The IDPS CTP algorithms are described by *Wong et al.* [2009] and in the ATBDs (see reference links in Appendix A). The IDPS uses multiple approaches for CTP generation. During the day, CTP is estimated simultaneously with COP. For nighttime, COP and CTP are estimated simultaneously but with an IR–only approach. For daytime water clouds, a different method is applied that involves the IR-window channel estimation of CTP assuming an opaque cloud. This approach therefore differs from the NOAA PATMOS-x (GOES AWG) and MODIS MOD06 approaches that employ an IR-only approach to achieve day/night consistency. The CTP algorithms operate on the VIIRS M-band observations (750 m) and generate the VIIRS IP values. The VIIRS EDRs are generated through an aggregation process that is not well understood. For reference, JPSS requirements specifications for accuracy, precision and coverage for CTP EDRs are given in **Table 3.1**. Accuracy is defined as the bias of the distribution of truth minus retrieved, precision is the standard deviation of that distribution, and coverage represents the global area that must be covered per day. The "Coverage" specification is interpreted as the percentage of cloudy pixels with a successful retrieval. **Table 3.1** provides the specifications for two conditions based on cloud optical thickness. Note that specifications for cloud-top height and temperature are more stringent for clouds with optical thickness (COT) greater than 1.

Table 3.1. For context, JPSS VIIRS Cloud-top EDR specifications.

Cloud-top EDR	Accuracy	Precision	Coverage (%)
Height	2 km (COT<1), 1 km (COT>1)	2 km (COT<1), 1 km (COT>1)	90
Pressure	100 mb (COT>1) & 0-3 km, 75 mb (COT>1) & 3-7 km, 50 mb (COT>1) & >7 km	100 mb (COT>1) & 0-3 km, 75 mb (COT>1) & 3-7 km, 50 mb (COT>1) & >7 km	90
Temperature	6 K (COT<1), 3 K COT>1	6 K (COT<1), 3 K COT>1	90

Issues with use of CTP CDRs from IDPS: The cloud mask section lists multiple issues with the stability of the IDPS that limit the utility of any IDPS products to serve as CDRs. Those issues are also relevant here and will not be repeated. There are several Specific CTP issues with the IDPS are listed below.

- The IDPS CTP/CTH product is an aggregation of four different retrieval algorithms which are selected as a function of both cloud phase and day/night with each method having different sensitivities and biases. This results in significant day/night differences in the CTP climatology as presented in Figure 3.3.

- Unlike MODIS, the IDPS algorithm performance is highly dependent on accurate cloud phase selection which is retrieved by the VCM (cloud mask) making the products very sensitive to the upstream (VCM) performance.

- The IDPS CTP is not retrieved for probably cloudy pixels. This significantly biases the CTP results to optical thick clouds.

- The use of the reflectance channels in the IDPS CTP algorithm creates significant instabilities in the resulting CTP due to the complexity of accurately characterising the cloud radiation in the visible.

- The CTP algorithm uses NWP profiles to compute clear-sky radiance and transmittance profiles and to convert retrieved temperature to pressure and height. The IDPS uses NWP data from NCEP/GFS and NRL/NOGAPS. NWP models are undergoing constant evolution and do not offer a stable data source suitable for CDR generation. Ancillary data for CDR generation needs to be stable and come from Reanalysis or other consistent sources.

- Various attempts to run the CTP codes outside of the IDPS have failed to date. The cost to extract the IDPS CTP code to run outside of IDPS is unknown.

3.2 Evaluation Methodologies

An evaluation of CTP performance from the first year of operation is presented. This section has two main components. The first conducts a detailed analysis of the IDPS VIIRS CTP IPs through comparison with the CTP products provided by NASA A-train sensors (MYD06 CTP and active sensor measurements from CALIPSO and CloudSat). The active sensor provides high accuracy but for only a specific (and very narrow, about 80 m cross-track for CALIOP) portion of the imager swath. Imager–to–imager comparisons cover a large range of viewing angles. These comparisons are complementary and are sufficient to assess the current VIIRS cloud products with respect to the other operational sensors. The second component focuses on the VIIRS CTP EDRs rather than the IPs. The EDR evaluation shows that in addition to pixel-level problems, there are additional issues in the aggregation process that cannot be resolved given the state of the EDR documentation available.

While the match-up periods between CALIPSO and VIIRS occur for a brief period (about 12 hours every 3 days), global coverage is provided over a period of months as shown in **Figure 3.1**. Figure 3.1 shows the intersections between VIIRS and CALIPSO for the focus time period of the VIIRS evaluation (May – September 2012) using a time difference threshold of ±20 min. The consistent pattern of coincidence results from the very similar orbital characteristics of NPP and the A-Train. As previously mentioned, the match methodology is documented in *Nagle and Holz* [2009].

A pictorial example of the physical collocation between VIIRS and CALIOP is presented in **Figure 3.2**. The VIIRS cloud products are retrieved at the pixel level (IP) and then averaged to the EDR product scale as specified in the contract. We note that the process adopted in the IDPS software to build the VIIRS EDRs from the IPs is unclear and unsupported in the documentation. That is, it is unclear what decisions are made and what filtering criteria are adopted in developing the EDR products. For this reason, we cannot replicate the EDRs from the IPs to better understand the IDPS cloud products. Because of our lack of understanding of the EDR aggregation process, we instead focus on the pixel–level

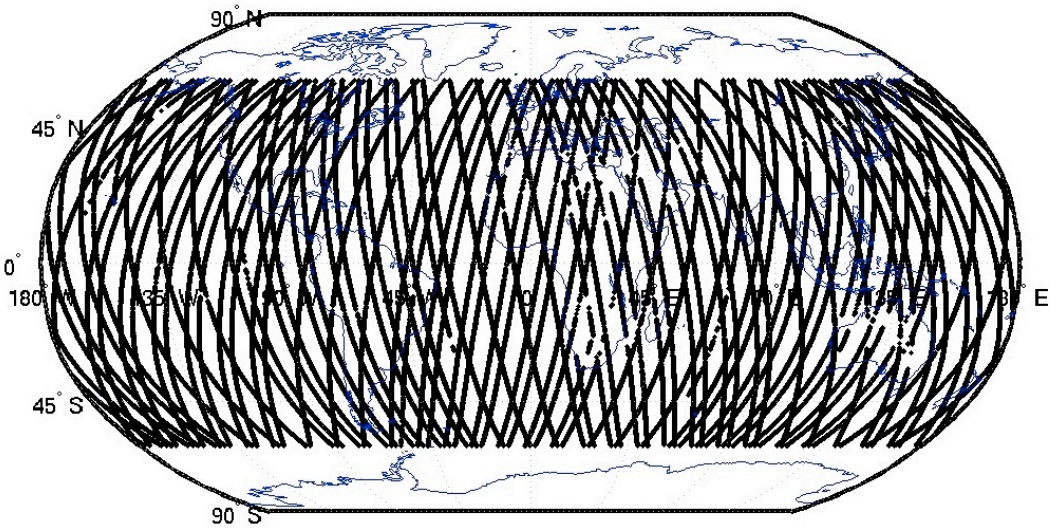

Fig. 3.1. The location of coincident VIIRS and CALIPSO observations with coincidence defined as 20 minutes between viewing the same location. Notice the very regular pattern of intersections.

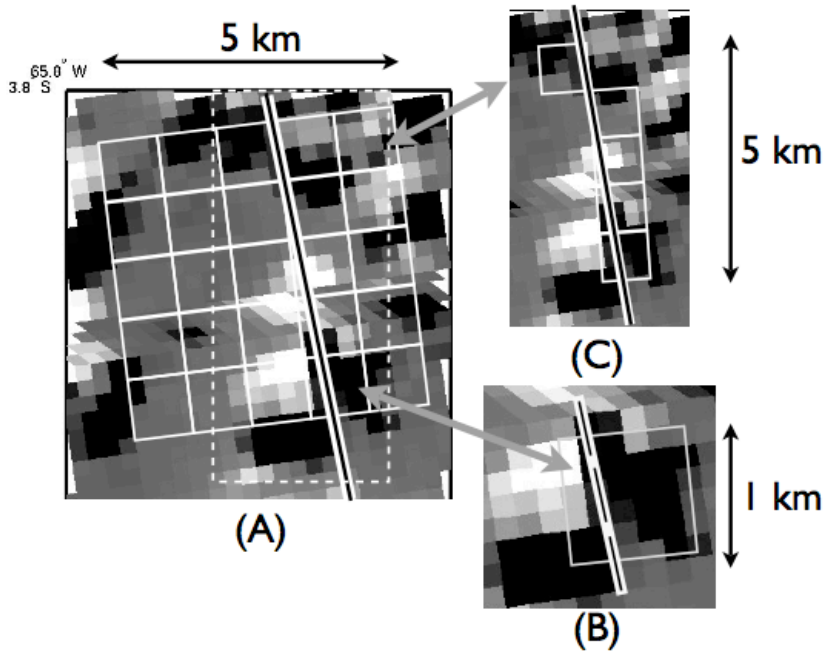

Fig. 3.2. Collocation geometry between CALIOP and VIIRS. Panels (a) and (c) present the EDR scale resolution with panel (c) presenting an approximate 750 meter resolution IP collocation. The image background image depicts sub–pixel cloud features.

retrievals provided in the IP products. This reduces complications in interpreting the impact of the EDR aggregation. As shown in **Fig. 3.2**, the spatial characteristics of the CALIOP surface footprint are approximated as a 80–meter wide line projected onto the Earths surface with the length of the line a function of the averaging used to generate the CALIOP cloud products. The CALIOP-VIIRS collocation process for the period between May 1–August 11 2012 resulted in a total of over 1.8 million cloudy-sky collocated match-ups.

The CALIOP V3 cloud layer products (CLay-Prov_V3-02) and the cloud profile product (CPro-Prov-V3-02) are used in the comparisons. For CTH, the CALIOP 5 km resolution product is used rather than the higher-resolution product. Although this does oversample the VIIRS IP resolution, it provides improved signal to noise (SNR) and lower uncertainties for the CALIOP cloud retrievals. For the CALIOP CTH evaluation, we use the Cloud Layer Top Altitude and the cloud feature classification product that provides cloud phase information. The cloud top height resolution for CALIOP is 60 m [*Winker et al.*, 2007]. Use is made of the VIIRS Quality Assurance (QA) information provided as part of the IP CTH retrieval. The QA provides information about retrieval convergence and identifies the retrieval method. The VIIRS CTH algorithm has four discrete retrieval methods that are selected as a function of day/night and cloud phase. As part of the evaluation we separate the analysis as a function of the retrieval method noted in the QA.

3.3 Evaluation Results

Comparisons with CALIOP

Figure 3.3 presents the histogram of difference between the VIIRS IP and CALIOP CTH retrievals separated by retrieval methodology for approximately 5 months of global observations. The CTH differences are presented in terms of (VIIRS-CALIOP) so that a positive difference means that VIIRS has a higher CTH than CALIOP. Similar comparisons between MODIS and CALIOP (MODIS-CALIOP) indicate that optically thin high clouds (e.g., cirrus) tend to have a bias of 1-2 km because cirrus tend to be geometrically thick but optically thin, and a passive radiance retrieval tends to place the cloud-height at the depth where the integrated optical extinction is approximately equal to unity. In this situation, CALIOP observes the uppermost boundary of the cloud layer while the passive imager is more indicative of an optical depth into the cloud, leading to a negative bias.

The CALIOP 5 km CTH product has both a very low uncertainty and high sensitivity (60 m). Other than a small random component of uncertainty resulting from the spatial and temporal sampling differences between CALIOP and VIIRS, the biases presented in **Figure 3.3** translate directly to biases in the VIIRS CTH. The combined distribution of all CTH retrievals (solid black) is bimodal with a very defined positive peak at +(2-3 km) and a second peak with a –(3-4 km) difference. The positive peak denotes cases when the VIIRS CTH overestimates the cloud top height relative to CALIOP. The separation of the biases as function of the VIIRS retrieval in **Figure 3.3** reveals a clear relationship between the cloud retrieval methodology and CTH biases compared to CALIOP. **Table 3.2** presents the global mean and standard deviation of the differences between VIIRS IP and CALIOP for the four retrieval paths.

For both (day/night) the water (low cloud) retrievals systematically overestimate CTH with the nighttime mode of the distribution at approximately +2 km. The day water cloud retrieval also has a positive bias although slightly smaller. Based on these results, we further investigated the retrieval algorithm and identified a clear deficiency in the CTH-P retrieval that may explain this bias. We found that the CTH-P algorithm does not correctly account for the frequent temperature inversions in the lower atmospheric resulting in the algorithm

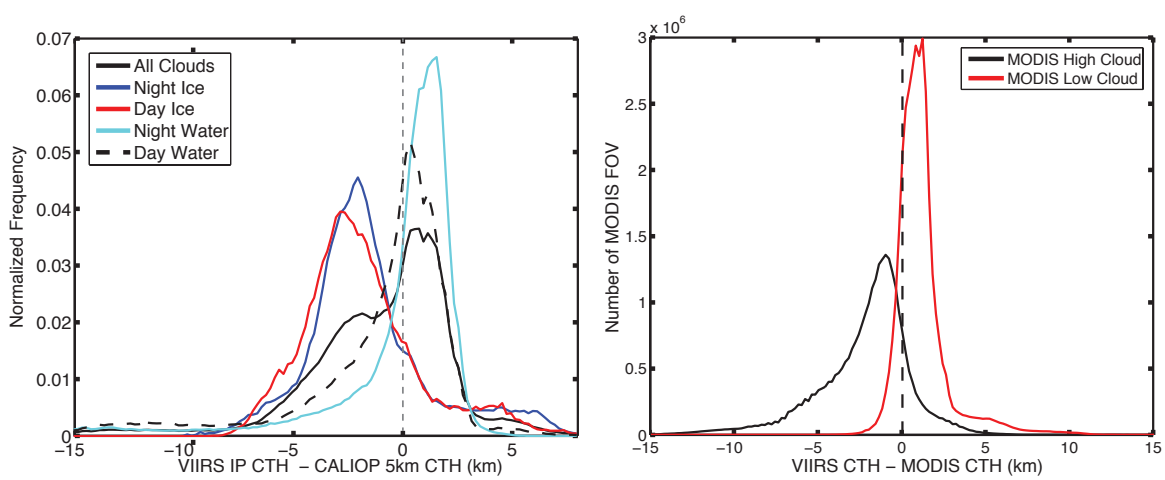

Fig. 3.3. (a) Global distribution of CTH differences between CALIOP and VIIRS IP retrievals. Results are separated by VIIRS retrieval method. Negative differences translate to VIIRS underestimating the CTH. (b) Differences between pixel-level colocated (±20 min) VIIRS IP and MODIS CTH retrievals for a latitude zone of ±60° on 2 September 2012 (day and night observations). The IP heights show different biases for high and low clouds (according to MODIS CTP channel method).

Table 3.2. Mean and standard deviation of biases relative to CALIOP separated by retrieval type. Negative values occur when VIIRS underestimates CALIOP.

	All Retrievals	Night, Ice	Day, Ice	Night, Water	Day, Water
Mean (km)	-0.9	-1.5	-1.8	-1.8	-1.1
STD (km)	3.4	2.9	2.7	3.3	3.7

incorrectly relating cloud top temperature to CTH. In addition to the positive bias there is also a negative bias in the water cloud retrievals in **Figure 3.3** with the negative tail extending to -10 km.

The ice cloud retrievals for day and night are presented in the figure as the red and blue solid distributions. Surprisingly the day and night performance is similar despite using different spectral channels and retrieval methodologies. Both ice cloud retrievals demonstrate a negative bias (lower VIIRS CTH) relative to CALIOP with the peak in the distribution between 3-4 km lower than CALIOP. There is also a significant overestimation of the CTH with a positive tail for a significant fraction of the VIIRS-CALIOP match-ups with biases as large as +8 km relative to CALIOP. One cause for these cases could be that when the CTH-P retrieval does not converge and as a result selects the tropopause as the cloud top height. Another cause could be the presence of low-level water clouds beneath the upper-level cirrus; in such cases, the inferred CTH lies between the upper and lower cloud layers. Some amount of low bias in the distribution is not unexpected due to the different inherent sensitivity differences between CALIOP and a passive imager such as VIIRS. That being said, the underestimation of VIIRS is larger than we would have expected and deserves further investigation.

The regional dependence of the CTH-P retrievals is provided in **Fig. 3.4** on a 5˚x5˚ equal-angle grid. CTH differences are aggregated in each grid cell, from which are calculated the mean and standard deviations of the CTH differences between CALIOP and VIIRS. The results are separated by optically thin (COT < 1, left column) and optically thick (COT > 1, right column). The figure demonstrates that there is a strong regional dependence on the VIIRS CTH-P performance with the results strongly correlated by the dominant cloud regimes for each region. The areas of bright red over ocean in the figure (VIIRS over estimating the CTH) occur in regions dominated by stratocumulus or mid–level clouds. However, there is also a CTH overestimation over the Tibetan Plateau and also over other high-elevation terrain. Behavior of the VIIRS CTH algorithm needs further investigation over high-elevation terrain, and also over regions with sparse vegetation such as South Africa and central Australia. Conversely, the underestimation of the CTH for ice clouds occurs primarily in the Tropics and also over the high-elevation terrain in Antarctica. The non-opaque ice cloud analysis will have only so much accuracy with only the VIIRS IR-window channels being used for the CTH. An improvement in the CTH could arise through two avenues: (a) for daytime, use of the 1.38-μm channel could improve the ice cloud retrievals, and (b) use of the CrIS hyperspectral IR absorption channels to infer mid-to-high level CTP/CTH for both day/night conditions.

As a metric for these results, we summarize the CTH evaluation results in terms of the JPSS performance specifications presented in **Table 3.1**. From the gridded results presented in **Fig. 3.4**, we calculate the percent of the 5° grid boxes that meet the specifications. To account for the collocation uncertainty between CALIOP and VIIRS that is estimated to be less than 1 km, the precision requirements were reduced by 1 km (i.e., 3 km for COT < 1 and 2 km for COT > 1).

CTH CALIOP Comparison Summary:

- The VIIRS CTH retrieval demonstrates significant biases when compared to CALIOP.
- The CTH performance is strongly dependent on the algorithm selection, which in turn depends on cloud thermodynamic phase (e.g., day water or day ice).
- For ice clouds, the retrieval can both significantly underestimate and overestimate the CTH when compared to CALIOP. For cases of overestimation, we suspect the algorithm does not converge on a valid solution and instead selects the tropopause as the CTH. The large underestimation likely is combination of algorithm performance issues and sensitivity differences between the active and passive observations (CALIOP vs VIIRS).
- For low to mid-level clouds the algorithm systematically overestimates CTH.

The previous analysis evaluated the pixel-level IP cloud-top height. However, the IP product is not intended for use by the general community. Rather, the CTP EDR is the official product made available to the community through CLASS. Aside from our previous comment that the EDR aggregation is not documented, we did assess the VIIRS pressure EDR using products from May 1, 2012. While the IP QF value for cloud products are de-

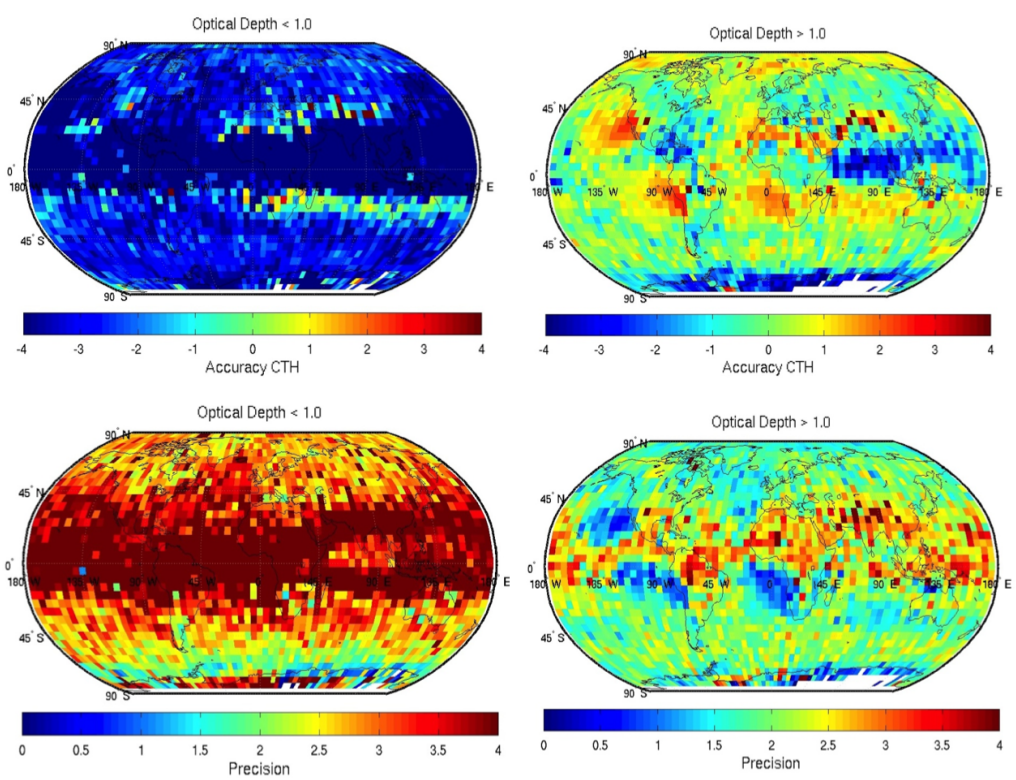

Fig. 3.4. The global distribution of CTH differences between CALIOP and VIIRS IP. The results are separated by the VIIRS COT retrieval (see Table 3.1). Negative differences translate to VIIRS underestimating the CTH.

tailed but often confusing and lacking key information, the EDR QF's are standardised across all EDRs and easy to interpret. Each EDR provides a 4-level integer quality flag that represents the "Overall Quality" of the EDR. The difference in global gridded CTP with and without QF filtering is dramatic. Not surprisingly, our finding is that the user of the EDR product must use Quality Flags (QF) to properly use the product. Without the QF flags, users are very likely to misuse the product, potentially resulting in flawed analyses. Unfortunately, our experience with providing global cloud products is that users generally do not use quality flags, and if they do, they are not always used properly. As a result of our own lessons-learned, the Collection 6 COP Level-2 data sets are no longer using QA bits to isolate the key pixel populations.

VIIRS–MYD06 Comparisons

While global monthly gridded products exist for the MODIS cloud products (MOD08), there is no such product for VIIRS. To provide a consistent way to filter the cloud products similarly for different sensors, we developed a new approach for our gridded CTP assessment activities. The goal is to develop a method with which any geo-referenced parameter, at any level of processing (L1B/L2), can be projected from its non-uniform instrument domain to a uniform space-time domain. As such, the gridded output is tailored to specific research needs but is created for a user-defined (not product-defined) length of time, from any suite of instruments relevant to the study. Our approach is called the space-time gridding (STG) method and is documented in Smith et al. [2013]. The STG approach results in a daily gridded product at a user-selected spatial resolution. A longer–term global gridded product is developed in a subsequent step from the daily maps.

For the high cloud comparisons of global CTP shown in **Fig. 3.5**, results for the month of September 2012 are aggregated to a 1° grid. The data are filtered by CTP $\leq$ 440 hPa and viewing zenith angle $\leq$ 32°. For this comparison, we use the MODIS Collection 6 5 km CTP results provided by the Atmosphere PEATE. The VIIRS EDR product provides the corresponding 5 km CTP. The (MODIS-VIIRS) CTH difference plot indicates that in general, daytime MODIS cloud top pressures are about 50 hPa lower than those from VIIRS, with larger differences (about 100 hPa) in the nighttime comparison. At the level of ice clouds in the troposphere, a rule of thumb is that 1 km corresponds to approximately 50 hPa. Thus there is a bias in high-level cloud heights between MODIS and VIIRS, with VIIRS CTH generally lower than MODIS. This is not always the case, however. For example, the opposite it true for the daytime over the Himalayas and the Tibetan Plateau, i.e., MODIS CTP values are higher than VIIRS (lower heights). This raises a red flag because of inherent retrieval difficulties over high elevation terrain/mountains. **Figs. 3.6** and **3.7** show comparisons for mid- and low-pressure clouds, respectively. Mid-pressure differences are characteristically similar to **Fig. 3.5** though more significant for the daytime retrievals, while low-pressure differences show a reversal of sign (MODIS with lower cloud altitudes) with large differences over the oceans being indicative of VIIRS biases in the presence of strong boundary layer inversions [*Ackerman et al.*, 2008; *Holz et al.*, 2008].

Context: the GEWEX Cloud Assessment

One of the main achievements of the cloud climate community over the last several years has been the completion of the first version of the GEWEX Cloud Climatology Assessment Report [*Stubenrauch et al.*, 2013]. This report conducted uniform analyses on the various cloud climate data sets that were in existence. These included the EOS/A-Train

data from MODIS, MISR and AIRS, the multi-decadal records from AVHRR and HIRS and the blended geostationary data from ISCCP. One benefit of this effort was the generation of benchmark metrics that can be used to quickly assess if a new data set falls with the values of the existing climatologies.

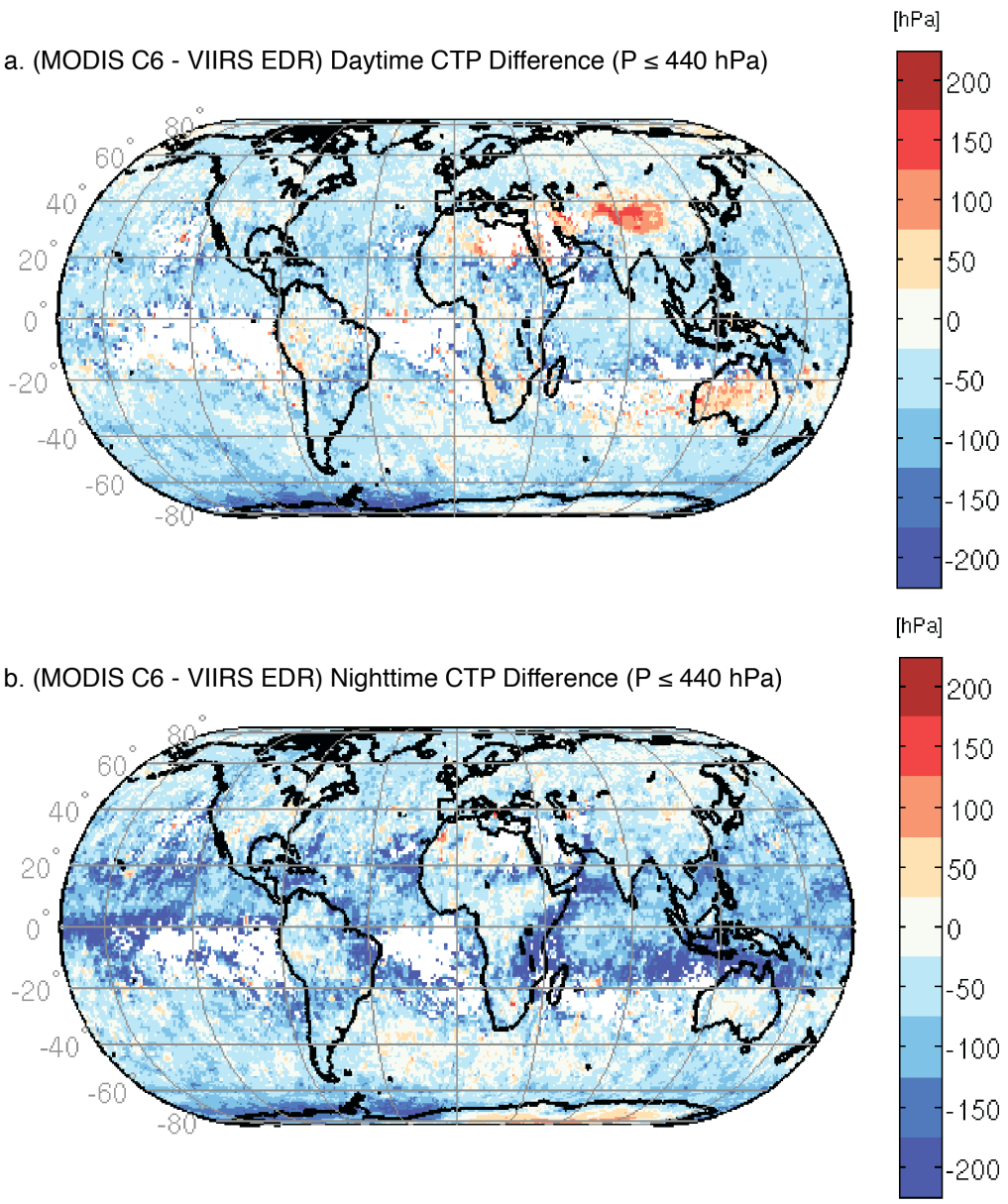

Fig. 3.5.Results for high-altitude cloud top pressures (CTP ≤ 440 hPa) differences between MYD06 Collection 6 5 km CTP and VIIRS 5 km EDR CTP for the full month of September 2012. Cloud top pressure (in hPa) is presented on a 1° equal-angle grid for the (MODIS–VIIRS) differences for (a) daytime and (b) nighttime.

Figure 3.8 is taken from the GEWEX Cloud Report and shows the global mean cloud amounts and their relative distribution in high, mid and low layers from the participating data sets. In this analysis, the cloud layer is defined by CTP with high clouds having CTP < 440 hPa and low clouds have CTP > 680 hPa. The sensors most similar to VIIRS in terms of spectral content and observation geometry are MODIS (MODIS-CE, MODIS-ST) and AVHRR (PATMOS-x). Data from the IDPS VIIRS were compiled during November 2012 and plotted onto Fig. 3.8 as the horizontal red lines. To verify that November 2012 was not an anomaly, the PATMOS-x algorithm was also run on VIIRS SDRs (i.e., VIIRS_AWGMOD elsewhere in this document) and its results are shown as the horizontal blue lines.

Figure 3.8 confirms that the biases seen between the IDPS CTP and the C6 MYD06 or CALIOP are sufficient to impact the global mean IDPS VIIRS results. The cloud amount (CA) results are low because no CTP values are generated in the IDPS for pixels classified as probably-cloudy by the VCM. If the VIIRS cloud mask were used to generate CA, the re-

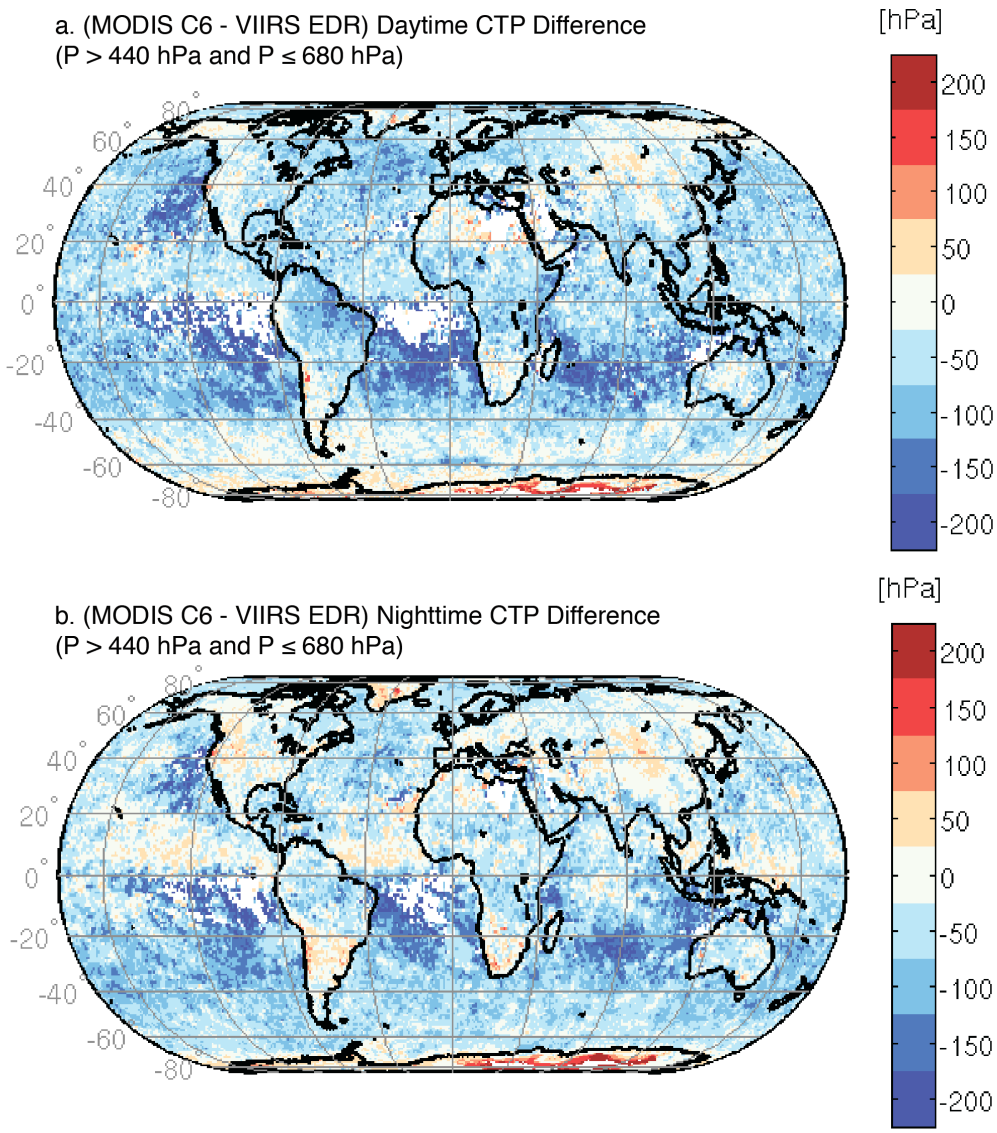

Fig. 3.6. Same as Fig. 3.5 but for mid-altitude cloud top pressures (440 hPa < CTP ≤ 680 hPa).

sult would be about 10% higher and lie within the expected range. However, for relative cloud amounts (CAHR, CAMR and CALR) to sum to unity, the CA value defined by the presence of CTP is required. While the CAHR is in family, the IDPS results have a CAMR that is higher than expected. The high CAMR values from ISCCP come from the lack of spectral information available to ISCCP for high cloud determination. VIIRS is expected to generate CAMR values similar to the MODIS and AVHRR values. The CALR value for VIIRS is also lower than expected and is likely due to overestimation of mid-layer cloud. While the IDPS VIIRS results are not the outliers, their performance in general is outside that expected for a VIIRS Cloud CTP CDR relative the GEWEX results.

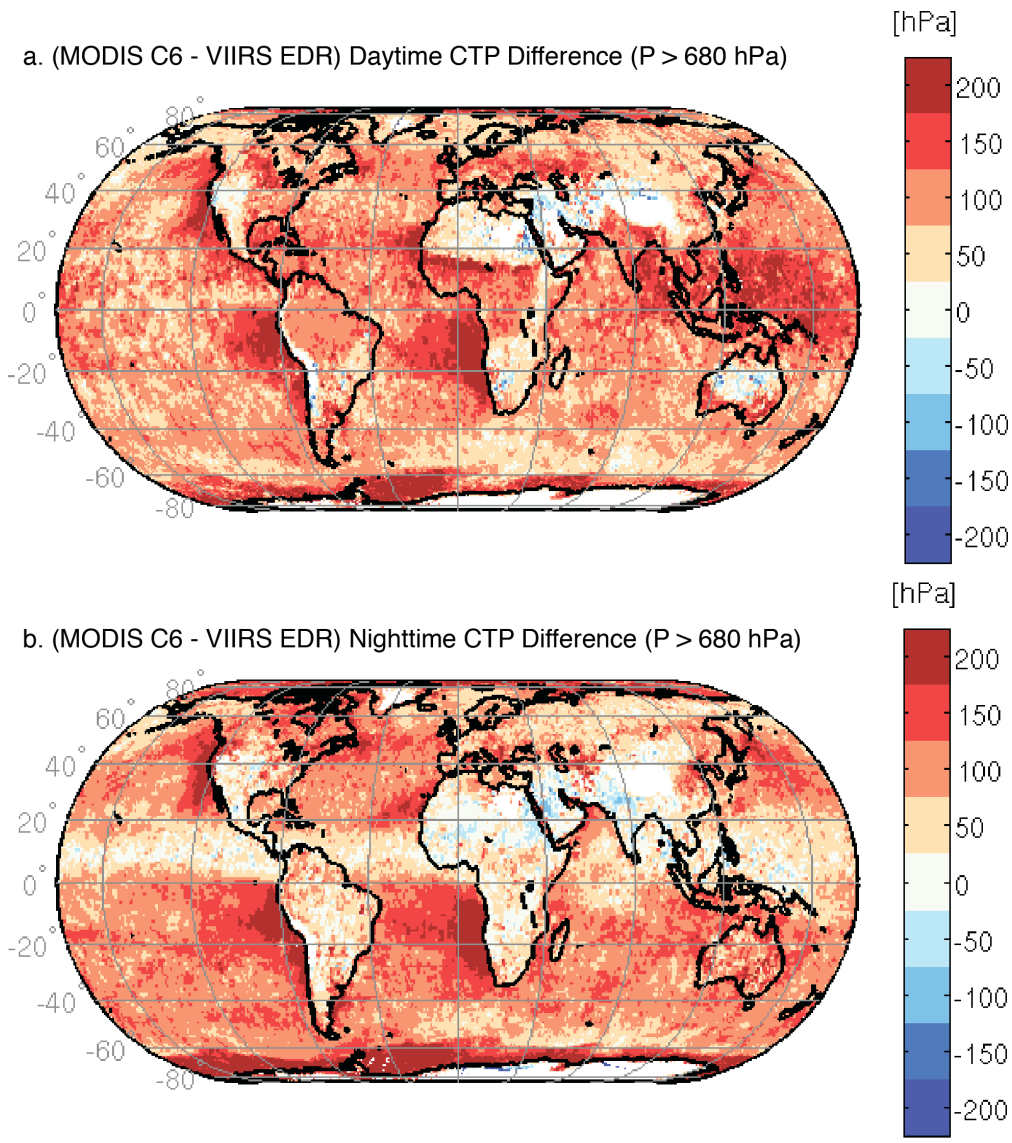

Fig. 3.7. Same as Fig. 3.5 but for low-altitude cloud top pressures (CTP > 680 hPa).

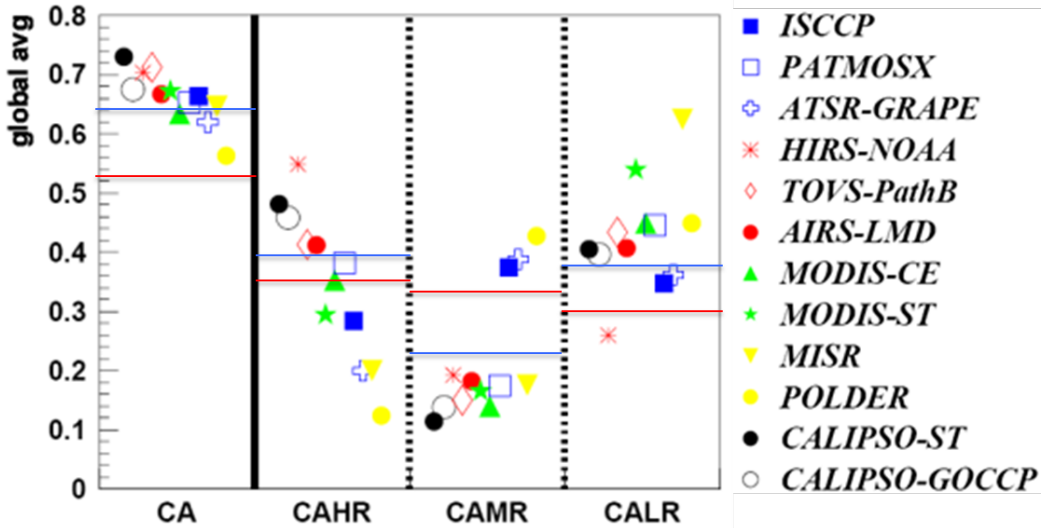

Fig. 3.8. Global mean total cloud amount (CA) and high-level, mid-level and low-level cloud amount relative to total cloud amount (CAHR + CAMR + CALR = 1). Statistics are averaged over daytime measurements (1:30 – 3:00 PM LT, except MISR and ATSR-GRAPE at 10:30 AM LT). Horizontal lines show VIIRS results. Horizontal red lines show IDPS VIIRS results for November 2012. Horizontal blue lines show PATMOS-x VIIRS results for November 2012. [from *Stubenrauch et al.*, 2013].

3.4 Conclusions

This section analyzed the potential utility of IDPS VIIRS EDRs to serve as CDRs. After a review of the algorithms and the IDPS-specific issues, a performance analysis was conducted. This performance analysis was based on detailed comparisons of VIIRS CTP against similar products from Aqua/MODIS and CALIOP. The main points that came out of this analysis are listed below.

- The VIIRS IP QF's are lacking information and confusing.
- While it is difficult to find the actual documentation of the VIIRS CTP quality flags in the EDRs, the documentation is at least straightforward to understand. Their application however introduces significant sampling biases that appear to be cloud-type dependent. This would hamper any attempt to make a useable CTP climatology.
- Compared to MODIS and CALIPSO, the VIIRS CTP does appear to have significant and cloud-type dependent biases. While some EDR errors are not fatal for CDRs, the magnitudes of these biases cause the VIIRS CTP CDRs to be out of family with existing operational cloud products.
- The Overall QF values seem to have errors (classifying land pixels in the oceanic glint zone as degraded) and cause scene-dependent and cloud-type dependent sampling biases if utilized.
- Analysis of the VIIRS EDR cloud-top pressures raises numerous questions with the aggregation process.

- We have been unable to run the VIIRS CTP algorithms in ADL outside of a limited number of test granules. We do not see a path forward using the VIIRS IDPS CTP code.

- Given the performance issues with the CTP EDR in the first year of NPP, we see no driving reason to extract the IDPS VIIRS CTP code and run it outside of the IDPS.

In summary, we conclude that NASA will need to adopt non-IDPS routines to produce suitable CTP data records from VIIRS. As mentioned elsewhere, NOAA has a non-IDPS VIIRS CTP algorithm (GOES AWG/PATMOS-x) that has already been coupled with the MODIS-like COP algorithm (VIIRS_AWGMOD). This algorithm should not suffer from most of the issues raised here and should allow continuity with MODIS if the algorithm is run on both instrument records (see discussion in Sect. 1.2/B). In addition, as shown in Sect. 5.2, the spectral differences between VIIRS and MODIS provide a rationale to pursue a combined VIIRS and CrIS solution for CTP CDRs.

4. Cloud Optical Parameters (COP)

4.1 Comparison of Key Algorithm Approaches: IDPS vs. MODIS

The MODIS MOD06 optical/microphysical retrieval algorithm primarily uses 6 visible, near-infrared, shortwave and midwave-infrared channels, along with several IR channels. The product includes: cloud retrieval phase based on a variety of solar-reflectance and IR observations and/or retrievals [*King et al.*, 2004, 2010]; simultaneous retrievals of cloud optical thickness and spectral effective radius (separately from 1.6, 2.1, ad 3.7 μm measurements), and derived water path [*Nakajima and King*, 1990; *Platnick and Valero*, 1995; *Platnick et al.*, 2001; *Platnick et al.*, 2003; *King et al.*, 2010] along with quantitative pixel-level uncertainty estimates for the above optical/microphysical retrievals [*Platnick et al.*, 2004]; Quality Assessment (QA) flags for filtering Level 2 data, including a Multilayer Detection Flag for use with effective radius retrievals [*Wind et al.*, 2010]; atmospheric corrections for above-cloud Rayleigh scattering [*Wang et al.*, 1997], ozone absorption, and water vapor attenuation (2.1 and 3.7 μm bands, in particular).

In addition to MODIS Level 1B data, the product currently relies on: the MODIS cloud mask and the cloud-top pressure portion of MOD06 [*Ackerman et al.*, 2008; *Holz et al.*, 2008], ice radiative models based on the particle spectral scattering calculations of *Yang et al.* [2005, 2007], and a variety of ancillary data sets, including temporal land surface spectral albedo derived from gap-filled MODIS C4 data [*Moody et al.*, 2005, 2007, 2008], snow/ice data from the Near-real-time Ice and Snow Extent (NISE), and forecast analysis fields (NCEP GDAS).

A number of significant updates to MOD06 have been implemented for C6 processing (details at: modis-atmos.gsfc.nasa.gov/products_C006update.html). C5 ice Look-up Tables (LUTs) used habit/distribution models from *Baum et al.* [2005] while C6 models are based on a single habit (severely roughened aggregated columns) that were chosen for consistency with IR cirrus optical thickness retrievals [*Holz et al.*, 2012]. QA and pixel filtering has been simplified with separate SDSs for the population of pixels expected to be partly cloudy and those that are more likely to be overcast. Sub-pixel heterogeneity derived from 250 m VIS/NIR measurements has been added as additional QA information. The C6 algorithm has updated the land spectral albedo map to use a gap-filled dataset derived from

Aqua/Terra C5 product (MCD43B3). Ocean LUTs now use a wind-speed interpolated Cox-Munk surface bidirectional reflectance model.

As summarized in **Table 1**, the IDPS optical retrieval uses the 1.6 μm channel during the day and the 3.7 μm during nighttime observations. MOD06 derives separate effective particle size and water path from the 1.6, 2.1, and 3.7 channels during daytime only. Therefore, only the daytime 1.6 μm size retrievals can be compared. Water path is not produced by the IDPS. The LUTs for both water and ice clouds are more complex than those used by MODIS because the VIIRS LUTs incorporate: (a) an atmosphere, (b) range of surface albedos (apparently parameterized from surface type information [ATBD 474-00042]), and (c) a constant aerosol loading. MODIS LUTs used for land and snow/ice retrievals are for a black surface and atmosphere-free loading. On a pixel-to-pixel basis, atmospheric corrections are incorporated and high spatial resolution land surface spectral albedo maps (mentioned above) are added using Lambertian assumptions. Over the ocean, LUTs using Cox-Munk reflectance models are calculated for three wind speeds and averaged over vector directions. While radiative scattering/absorption models used to develop the ice cloud LUTs for VIIRS are said to assume smooth and multi-habit particles in available documentation [ATBD 474-00042], it appears that the models of *Baum et al.* [2005] were adopted for a LUT change that was incorporated into IDPS processing in September 2012 (further details in Sect. 4.2). While the latter models are consistent with those being used in MODIS C5 processing, they will not be consistent with C6 processing as mentioned in the previous paragraph. The impact of different ice habit assumptions can result in significant differences in retrieved optical thickness and effective radius for measurements from the same instrument [*Yang et al.*, 2007; *Holz et al.*, 2012].

Even if the IDPS algorithm produced a 2.2 μm window size retrieval, there is a significant change in the spectral location for the VIIRS shortwave infrared band (from 2.13 μm on MODIS to 2.25 μm on VIIRS), resulting in significantly less absorption for VIIRS. The new spectral location results in a reversal in the relative absorption between liquid water and ice phase particles. This window channel provides the "standard" effective radius retrieval for MODIS that is used in Level-3 aggregations. Due to ice cloud vertical heterogeneity, it is unlikely that the two sensors will give comparable retrievals [*Zhang et al.*, 2010]. In addition, a near-infrared water vapor band (0.94 μm) used for multilayer cloud detection and optical retrieval quality flagging [*Wind et al.*, 2010] is not available on VIIRS. However, VIIRS does use other spectral channels for multi-layer identification that are common to the MODIS algorithm.

4.2 Evaluation Methodologies

As with other cloud products, the focus of the evaluation is on IP data sets at the native M-band (750 m) spatial resolution. Quality Flag (QF) filtering is consistent with filtering done for the Sect. 3 CTP analysis. The data were provided for two releases, one from the start of this project (version 5) and one for data released from 10 September 2012 (version 6).

The COP retrievals depend directly on the forward model LUTs). This is more of an issue with ice models, which need to adopt a set of habit(s) and surface roughness assumptions. It is difficult to separate issues caused by LUT from other retrieval algorithm differences. Therefore, in Sect. 4.3.1 we focus on the ice LUT differences only.

In Sect. 4.3.2 we provide comparisons of global IP aggregations vs. MYD06 and the ported MODIS COP code (VIIRS_AWGMOD). A common aggregation tool developed by R. Holz was used for all three COP datasets (IDPS IP, MYD06, VIIRS_AWGMOD). The MYD06 and VIIRS_AWGMOD 1.6 µm derived effective radii retrievals are aggregated for equivalence with the daytime IDPS algorithm. Aggregations included the entire swath for VIIRS and MODIS (maximum satellite view angles of 70.2° and 65.7° for VIIRS and MODIS, respectively).

4.3 Evaluation Results

4.3.1 Ice LUT comparisons

Daytime retrieval of cloud optical thickness and effective particle size from the nearly 13-year MODIS record have proven to be very useful for climate studies. These cloud optical property retrievals are performed by comparing measured reflectances at two selected channels, typically one absorbing and one non-absorbing, with simulated reflectances calculated using a radiative transfer model and assumptions about cloud microphysics, surface reflectance, and occasionally other parameters. The simulated reflectances are typically precomputed for a range of viewing geometries and surface conditions and are referred to as look-up tables (LUTs). In this section, we summarize comparisons between the MODIS and VIIRS IDPS ice cloud optical property LUTs.

We focus here on each instrument's 1.6 µm spectral window retrievals of effective particle size in our comparisons because this window channel is the only one used in the IDPS daytime effective particle size product. Note that the VIIRS 1.61 µm and MODIS 1.64 µm channels are spectrally close to each other (**Fig. 4.1**), more so than for the VIIRS 2.25 µm and MODIS 2.13 µm bands. VIIRS uses reflectances at 0.672 µm over non-snow/ice surfaces and 1.24 µm over snow/ice surfaces for cloud optical thickness retrievals while MODIS uses reflectances at 0.645, 0.86, and 1.24 µm for optical thickness retrievals over

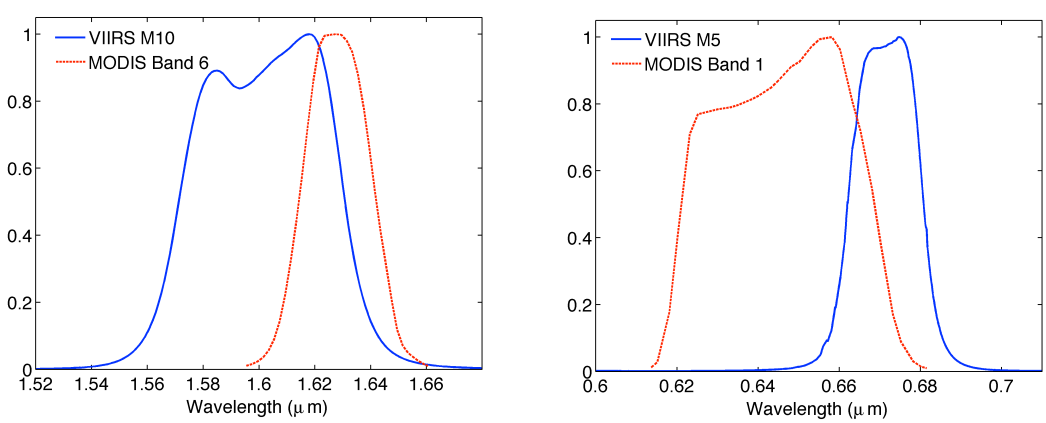

Fig. 4.1Comparison of VIIRS and MODIS spectral response function for cloud optical property retrieval bands. On the left are the VIIRS 0.672 µm (blue line) and MODIS 0.645 µm (red line) channels that form the basis of optical thickness retrievals. On the right are the VIIRS 1.61 µm and MODIS 1.64 µm channels that form the basis of the effective particle size retrievals.

land, ocean, and bright snow/sea ice surfaces, respectively. In this summary, we focus on each instrument's 0.6 µm retrievals of cloud optical thickness.

It is important to note that up-to-date technical information regarding the VIIRS cloud optical property retrievals is not available. Personal communication with Dr. Eric Wong from Northrop Grumman revealed that the JPSS VIIRS cloud optical property ATBD and Software documents available at http://npp.gsfc.nasa.gov/science/documents.html are not current and do not describe the current retrieval methodology and assumptions. While the ATBD describes ice cloud optical property LUTs based on a set of ice models developed by UCLA, according to Dr. Wong, the current VIIRS cloud optical property retrievals are instead using ice cloud optical property LUTs based on the thirteen ice cloud models from *Baum et al.* [2005] that are used in the MODIS Collection 5 (C5) retrievals. Dr. Wong helped us obtain the VIIRS LUTs current as of December 2012. Because of the lack of technical documentation regarding the VIIRS LUTs, we are unsure what differences from the operational MODIS C5 retrievals should be expected. Additionally, we are not certain that Northrop Grumman has implemented the LUTs correctly.

To evaluate continuity of cloud effective particle size and optical thickness retrievals, we compare three sets of LUTs: VIIRS IDPS, (MODIS) Collection 6 integrated over the MODIS spectral response functions, and (MODIS) Collection 6 integrated over the VIIRS spectral response functions. The VIIRS-IDPS LUTs are from Andi Walther at the University of Wisconsin Space Science and Engineering Center while the Collection 6 LUTs are from the GSFC MODIS cloud retrieval group (S. Platnick et al.). Comparisons for the following viewing geometry are shown: solar zenith angle = 30°, satellite viewing angle = 30°, and relative azimuth angle = 100°.

The left panel of **Fig. 4.2** shows the Collection 6 ice models applied to the VIIRS (in blue) and to MODIS (red) channels. The agreement between the optical thickness contours demonstrates that the differences between the spectral response of the MODIS and VIIRS 0.6 µm channels should have minimal impact on the continuity of COT as long as the same microphysical properties are assumed for future MODIS and VIIRS retrievals. The offset between the effective particle radius contour lines (horizontal for large COT) shows that the different 1.6 µm spectral responses may impact particle size record continuity. This bears further investigation. The right panel of **Fig. 4.2** shows the impact of different microphysical property assumptions on cloud optical property continuity. The VIIRS IDPS LUTs (blue) are compared with C6 applied to the VIIRS channels (red). The fact that that blue and red curves do not line up show that inconsistent microphysical property assumptions will lead to large differences in optical property retrievals.

Fig 4.3 provided further detail on the right panel of **Fig. 4.2**, showing the percent relative differences between the C6 ice models applied to VIIRS and VIIRS IDPS ice cloud LUTs for the same VIIRS reflectance pairs. The colors in the left panel show that the percent relative difference in optical thickness is greatest for large particle sizes and for large optical thicknesses. The very large differences along the borders of the plot are due to reflectances that are not represented in one of the LUTs. The right panel shows that the VIIRS IDPS LUTs systematically require an ice cloud be more reflective in the SWIR to retrieve the same particle size produced by the C6 ice model retrieval. Because particle size retrievals are important for linking aerosols to climate impacts, as well as for calculating cloud radiative impacts, it is important to prevent systematic retrieval biases introduced by inconsistent LUTs from being interpreted as real climate change signals.

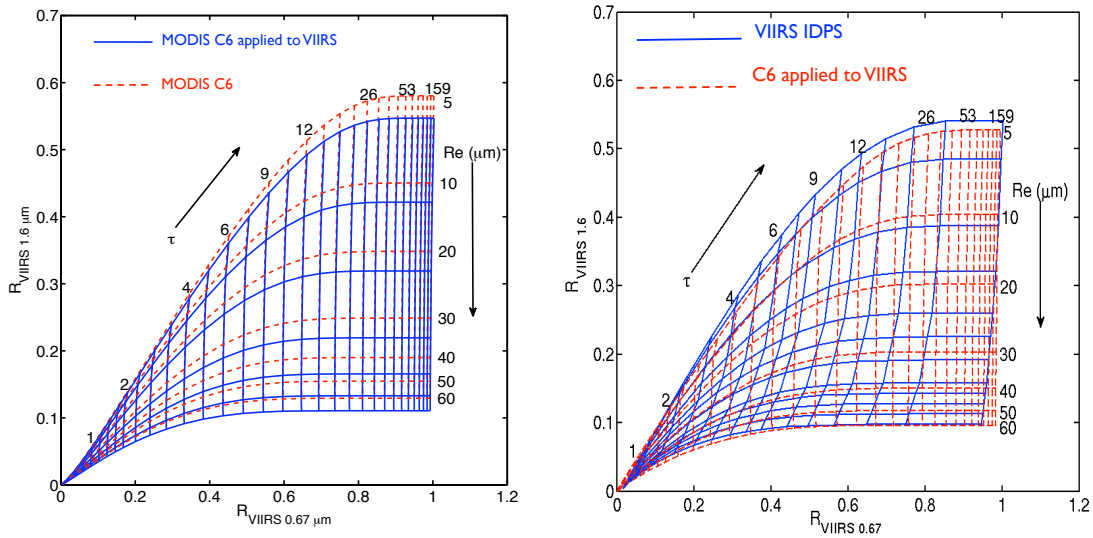

Fig. 4.2. Comparison of different MODIS and VIIRS LUTs for the following viewing geometry: solar zenith angle = 30°, satellite viewing angle = 30°, and relative azimuth angle = 100°. The numbers on the right side of the curves represent effective diameter values in μm while the numbers on the top of the curves represent optical thickness values and correspond to the red curves.

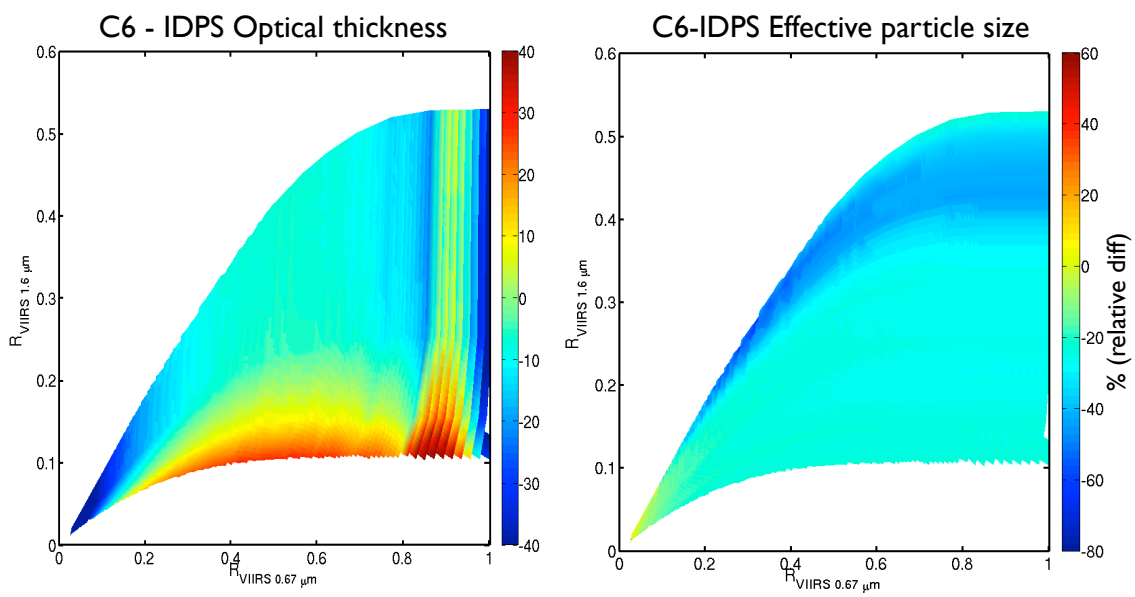

Fig. 4.3.The color shows the percent relative difference in retrieved optical thickness (left) and ice cloud effective particle size (right) between the MODIS C6 ice model applied to VIIRS and VIIRS IDPS LUTs for the following viewing geometry: solar zenith angle = 30°, satellite viewing angle = 30°, and relative azimuth angle = 100°. These figures correspond to the right panel of Fig. 4.2.

4.3.2 Retrieval comparisons

Here we show global gridded results for COT, CER for ice and water phases from the IDPS IP, the MYD06 product, and the hybrid heritage code run on VIIRS SDRs (VIIRS_AWG).

Figure 4.4 shows ice cloud mean COT and CER for September 2012 for all three products. The MYD06 and VIIRS_AWGCOT use the same LUTs and other algorithm details. The differences are that MYD06 uses MODIS cloud mask (MYD35) and CTP retrievals from MYD06; VIIRS_AWGMOD gets mask, phase, and CTP information from the AWG portion of the hybrid code. Nevertheless, the agreement between the two for both COT and CER is quite good, especially in comparison to the IDPS IP product (bottom panels) where there is an overall low bias in both CER and COT. Not shown is the similar pattern of ice cloud counts found by all products, including very low occurrence in the subtropical highs.

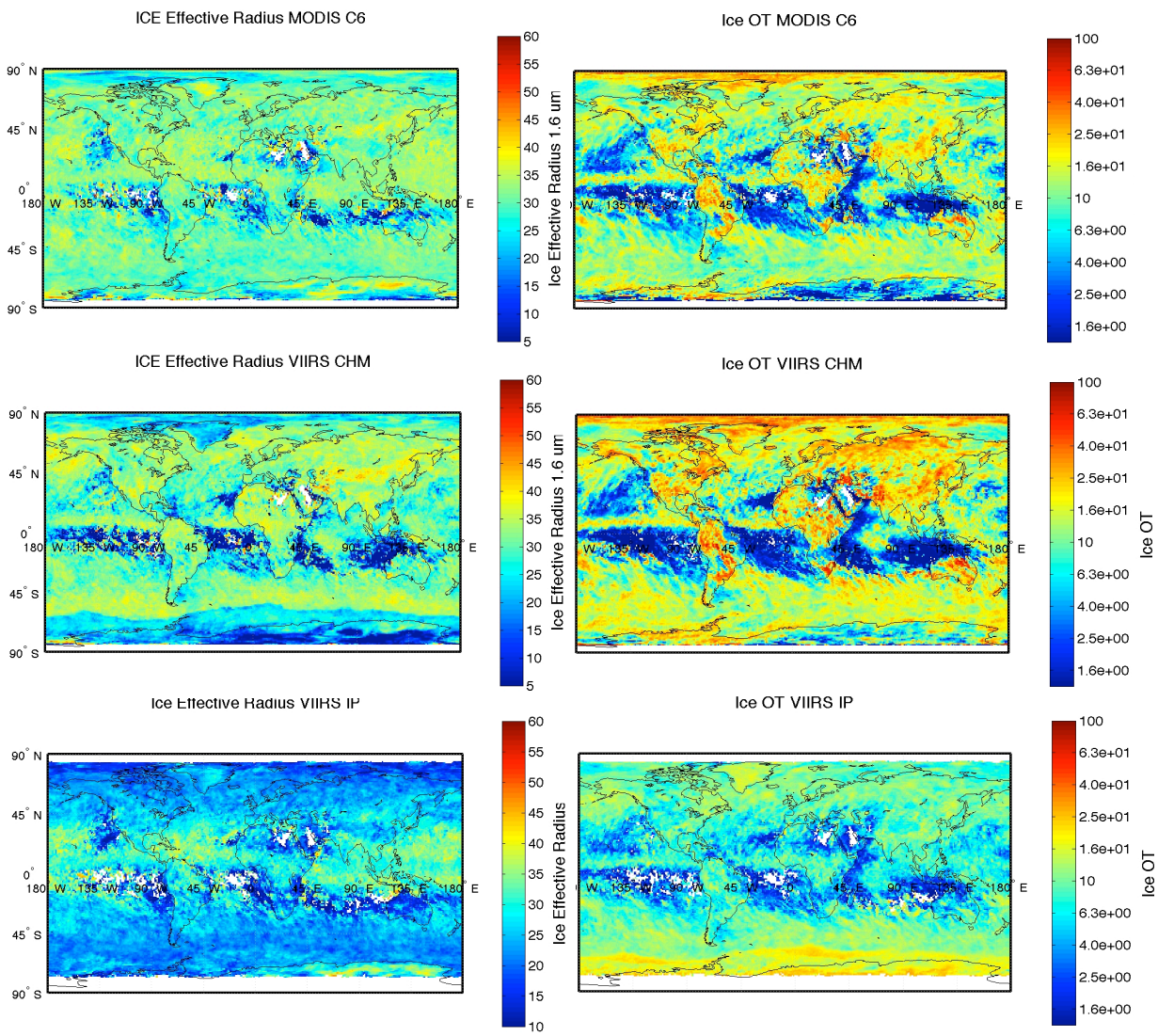

Fig. 4.4. Global September 2012 aggregation of mean ice cloud CER [μm] (left) and COT (right) from the C6 MYD06 (top), VIIRS_AWGMOD (middle), and IDPS IP products (bottom).

Figure 4.5 shows similar results for clouds identified as liquid water. Similar to the ice phase aggregations, the IDPS IP COT and CER means have a low bias relative to both MDY06 and VIIRS_AWGMOD, whereas the VIIRS_AWGMOD and MYD06 compare very favorably. Unlike for ice clouds, IP water CER are biased high overall compared with MYD06 or VIIRS_AWGMOD. It is unlikely that differences are related to water cloud LUTs which are relatively insensitive to size distribution details (unlike ice models). Our MODIS experience lends us to suspect that the IP's high CER and low COT bias could be indicative of inadequate filtering of partly cloudy pixels (both MYD06 and VIIRS_AWGMOD aggregations filter cloud edges, as well as partly cloudy pixels identified by MODIS 250 m cloud mask for MYD06). It may also be due to misidentification of ice clouds as liquid between IP and the other products. We also note the lack of water phase clouds being found near/over Antarctica for both the AWG and IDPS products. To help delineate regional discrepancies, mean differences are shown in **Fig. 4.6**.

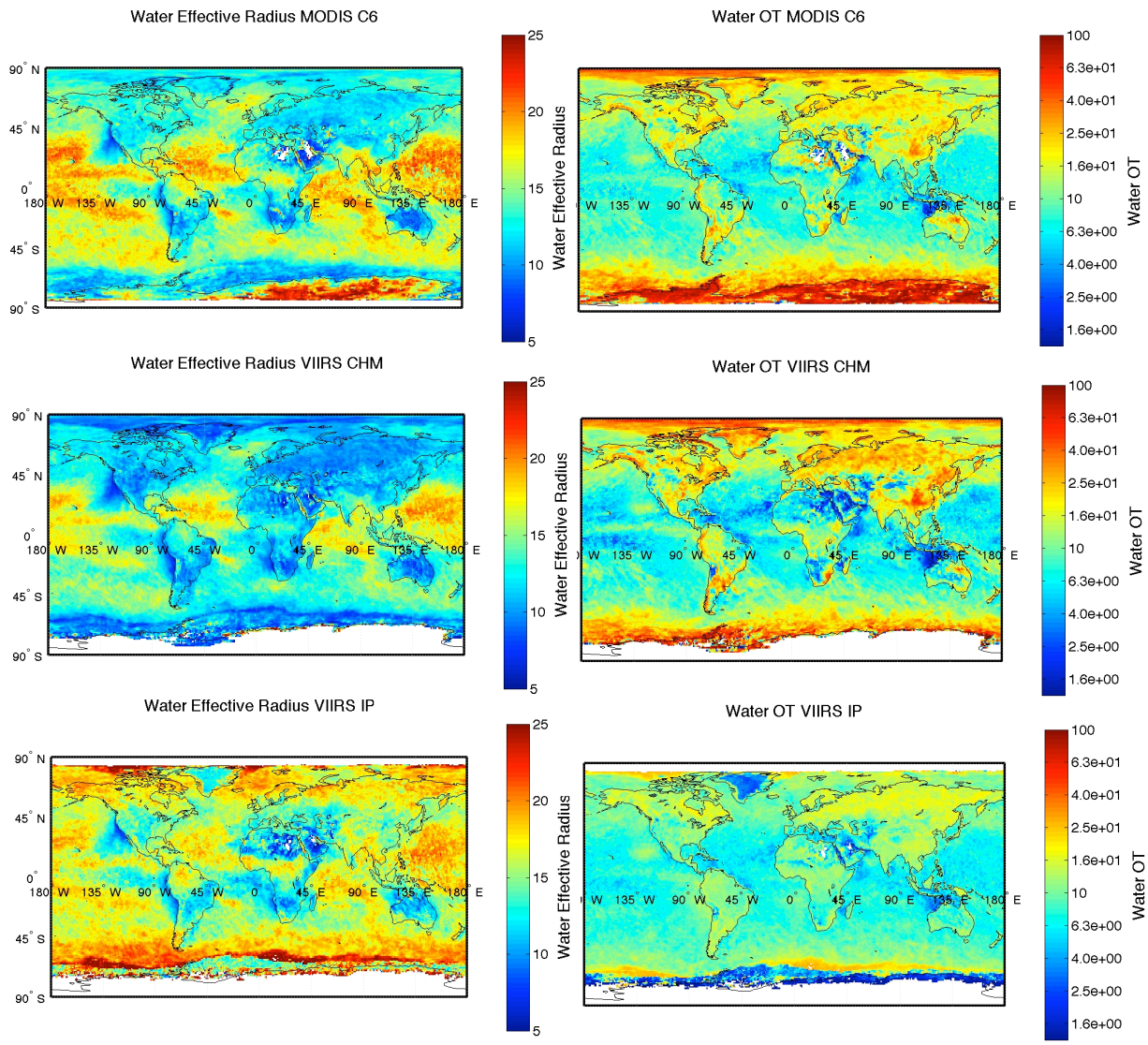

Fig. 4.5. Global September 2012 aggregation of mean liquid water cloud CER [μm] (left) and COT (right) from the C6 MYD06 (top), VIIRS_AWGMOD (middle), and IDPS IP products (bottom).

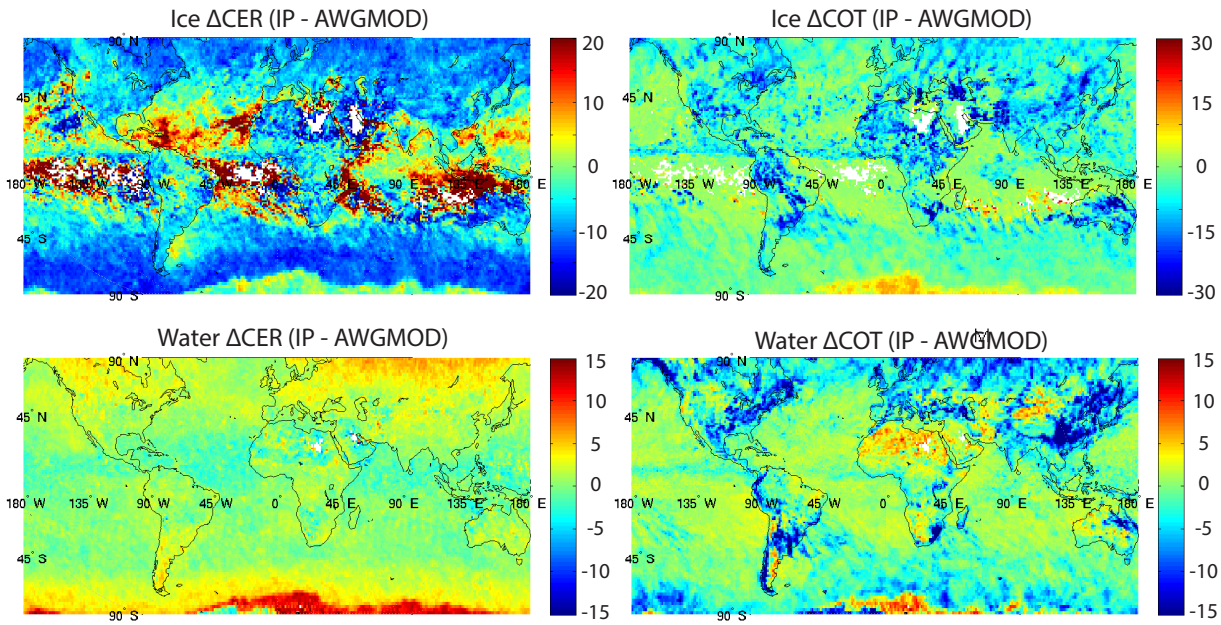

Fig. 4.6. Differences in IDPS IP global September 2012 aggregations of mean ice (top) and liquid water (bottom) CER [μm](left) and COT (right) relative to the team's VIIRS_AWGMOD product. The white regions (particularly in the ice difference images) indicates the absence of that particular phase in the two data sets.

Because of different explicit and implicit filtering (cloud detection, phase, partly cloudy pixel flagging, QA or QF filtering, different CTP and ancillary data (for IDPS), successful retrieval designations, etc.) it is difficult to isolate exact algorithm differences that result in the monthly mean discrepancies. We simply note that IP means are in general more biased relative to MYD06 than is the MODIS-like C6 algorithm adapted to VIIRS (VIIRS_AWGMOD). The next step in the pathway toward bridging MODIS and VIIRS COP records is to run the team's hybrid retrieval code on MODIS radiances (MODIS_AWGMOD), that is, not using the extra spectral information available from MODIS. This would achieve the goal of having a common algorithm as discussed in Sect. 1.2. The team will pursue this at the completion of this report.

4.4 Conclusions

From our analysis of IDPS IP products against MYD06 and the VIIRS_AWGMOD retrievals, we conclude that very significant differences exist between heritage and IP COP products. Based on these product comparisons alone (i.e., ignoring issues related to (re)processing), we do not see a viable path forward for the continuation of NASA COP data records via the IDPS algorithm. We recommend NASA adopt non-IDPS algorithms that will be under its development control in order to produce suitable COP data records from VIIRS. The cloud team's hybrid VIIRS_AWGMOD algorithm (GOES AWG/PATMOS-x

coupled with the MODIS-like C6 COP algorithm) provides a pathway as described in Sect. 1.2 and elsewhere.

We note the following specific limitations:

- Interpretation of the IP QFs is confusing and lacks the documentation necessary for proper use of the data (as for CTP). Filtering differences can have a significant impact on global gridded means.
- In addition to LUT and algorithm details, the quality of COP products depend directly on the quality of the cloud mask and phase algorithms. Differences in VCM and phase from heritage products will affect COP comparisons.
- IDPS ice LUTs are not consistent with MODIS C6 model assumptions. In addition, we note that analysis by the JPSS Cloud Cal/Val team came to the conclusions that the IDPS product still appears to have an issue in the calculation or use of the LUTs, even after the August 2012 IDPS update.
- The solution range of COT and CER is not optimal; the CER water cloud upper limit should be lower than 100 μm. The COT upper limit should be higher than 30 to use the full possible information content of the retrieval.
- Both COT and CER show strong angle dependencies in daily global maps and in individual granules.
- Histogram of COT and CER (not shown) display artificial discontinuities, appearing as either peaks or as an echelon (stair-case) shape [Figs. 6.7, 6.10 in *Heidinger et al.*, *JPSS Cloud Algorithm Assessment Report,* 2012].

5. Recommendations for the Way Forward

5.1 Achieving Cloud Data Record Continuity Across the MODIS/VIIRS Instrument Record

A practical definition of data record continuity for climate studies is the absence of climatologically significant bias in a data product across the instrument record that allows for quantitative climate change detection and analysis. As discussed in Sect. 1.5, significance for a cloud data record discontinuity is expected to be of order several percent depending on the spatial/temporal scale and the quantity involved. As a result, the time required to detect expected trends is a multi-decadal endeavour. The implications of having a break in the continuity of a climate record was also discussed.

The analyses of Sects. 1.6 and 2-3 show that differences seen between the IDSP IP product and heritage products (MOD35/MOD06 C5, C6) and heritage AVHRR/GOES/MODIS hybrid algorithms applied to VIIRS measurements (AWGMOD) produce discontinuities that are generally well outside the range required for climate science. And as shown in Sect. 1.6, the discontinuities are not merely fixed offsets that might be removed from the combined record, but rather have discontinuities that vary over the year indicating more complicated algorithm and/or instrument sensitivities. Collectively the analysis has shown

that both algorithm and instrument differences contribute to the discrepancies among the products.

Our primary recommendation is that, to the extent possible, Level-2 algorithm continuity should be an essential part of any NASA strategy for achieving long-term cloud climate data record continuity from EOS/MODIS into the NPP/JPSS era. In the case of cloud-top properties in particular, the absence of MODIS CO_2 absorption channels makes continuity inherently problematic. The algorithm-development that has been begun by the NPP cloud team (using common MODIS and VIIRS algorithms that can utilize the channel set of the more limited instrument) has provided a pathway for cloud data record continuity that can potentially bridge the MODIS and VIIRS sensors. It is recommended that ESD support the development and processing of such common sensor algorithms. The use of CrIS algorithms to account for the loss of VIIRS CO_2 shows promise as discussed further in the recommendations of Sect. 5.2.

The AWGMOD code discussed in this report is the foundation of the team's effort to build a common algorithm; modification of the code for use with MODIS measurement is expected by this summer. To help further demonstrate a feasible common algorithm pathway, the team is undertaking the development of a common cloud mask (referred to as VMCM) that is expected to be ready for testing in the next few months. The AWGMOD and VMCM codes will be merged when appropriate. The development of a common cloud phase algorithm based on MODIS C6 or AWG is straightforward if only IR channels are used. Inclusion of SWIR channels (as is done in MOD06 but not the IDPS algorithm) can perhaps be achieved if the spectrally unmatched 2.2 μm SWIR window channels are not used.

We emphasize again that climate record continuity and instrument/retrieval advancements are complimentary endeavors, that the common algorithm approach recommended for establishing a multi-decadal MODIS/VIIRS climate record does not mean that NASA should not move forward to obtain improved instrument measurement capabilities and derived physical records to improve our understanding of processes that define the climate system. Nor does a common algorithm approach mean that ESD should abandon support to refine and maintain cloud products for the most spectrally capable instrument (MODIS) as long as sensor performance allows.

Management and stewardship of Level-2 algorithms is a necessary but not sufficient condition for achieving data record continuity. In order to have control over the quality of NASA-supported geophysical products, *it is critical that ESD provide for its own calibrated and geolocated records, i.e., pixel-level instrument data records (Level-1B). Likewise, it is recommended that ESD support a production system capable of reprocessing NASA-supported NPP data record*s. The processing system should be tasked to work directly with NASA-funded algorithm developers, and should be scoped for algorithm development and testing in addition to routine production and distribution.

5.2 Improving Cloud Top Parameters/Phase with CrIS and VIIRS Observations

To develop cloud top climate data records, we need to work towards developing a seamless product dating to the beginning of the AVHRR and HIRS record (about 1980). No matter what future sensors provide data, we need to be able to efficiently append the decadal cloud top property record using the best available algorithms and calibration tech-

niques. With the exception of MODIS, the imagers alone (i.e., AVHRR and VIIRS) are limited in the IR spectral coverage to window measurements; neither AVHRR nor VIIRS have any IR spectral bands located in H_2O or CO_2 absorption regions and this will affect the inference of cloud top properties [*Heidinger et al.*, 2010]. Heidinger et al. discuss the consequences of that decision on the ability to estimate the cloud-top pressure (in this section, CTP will be used in regard to pressure, not parameters) for optically thin high cloud (cirrus). This study demonstrates that the ability to infer cirrus cloud top pressures/heights will be improved with sensors that include even a single absorption band. That is, VIIRS and AVHRR provide multiple IR window measurements that are used to infer cloud top pressure/height, but the inclusion of even a single absorption band will greatly improve the solution space for an optically thin ice cloud. *Heidinger et al.* (2010) show that for an example scene containing optically thin cirrus, the spectral bands used by the operational VIIRS algorithm [*Wong et al.*, 2007] provide a solution space of over 200 hPa. With the inclusion of the single CO_2 band at 13.3 μm, however, the solution space narrows to less than 30 hPa. The issue is not the algorithm but one of information content.

To state this more explicitly, the cloud top pressure from VIIRS alone can be improved significantly by supplementing with the information content from CrIS data. One possible approach is provided in Weisz et al. [2012]. The retrieval of CTP is provided by a dual-regression technique that has been fully tested on numerous case studies as well as on global data. The dual regression software is available as a standalone algorithm in the CSPP (Community Satellite Processing Package) at the University of Wisconsin-Madison. The effort to combine the information content from a sounder and imager is worth pursuing, and was demonstrated more than 20 years ago for AVHRR and HIRS [*Baum et al.*, 1992]. A long-term goal is to build a climatology based on merged data from both imager (e.g., AVHRR or VIIRS) and sounder (e.g., IASI or CrIS). The groundwork for such an approach is provided in *Weisz et al.* [2012]. This approach is applicable to morning orbit data from the MetOp-A/B platform and the afternoon orbit data from the JPSS. In fact, effort can also be adopted for the longer-term cloud climatology by combining AVHRR and HIRS, which to date have been paired on the NOAA operational platforms.

To demonstrate the potential information content provided by CrIS, **Figure 5.2.1** shows high cloud CTP differences between VIIRS EDRs and CrIS dual regression retrievals (referred to as the CrIS_CTP_DR algorithm in appendices and elsewhere) for September 2012 (a full month). The space-time gridding approach of *Smith et al.* [2013] is used to generate the monthly averaged CTPs for each sensor on a 1˚x1˚ equal angle grid for both daytime and nighttime results. There are several issues to note here. First, there is a general bias with the VIIRS CTP results for high-level clouds, i.e., ($P \leq 440$ hPa); VIIRS has the CTP too large putting the height too low (pressure and cloud height are inversely related). The bias is greater for nighttime than for daytime. Note that VIIRS has a different algorithm for nighttime and daytime ice clouds. While not shown, the frequency of high clouds in the VIIRS EDRs is much lower than for either MODIS or CrIS. Another issue is that part of the CTP day-night difference may result from the VIIRS EDR cloud phase assumed in the retrieval process. Regardless of the cause, or causes, of the differences, the CTP differences between CrIS and VIIRS approach 150-200 hPa. With the yardstick of 50 hPa ~ 1 km for high-level clouds, this indicates cloud top height differences of up to 4 km especially in the Tropics.

Figure 5.2.2 show the high-level cloud CTP differences between the gridded MYD06 C6 5 km product and CrIS for September 2012. The monthly averaged CTPs for each sensor are shown on a 1˚x1˚ equal angle grid for both daytime and nighttime results. Over much of the globe, the differences between CrIS and MODIS MYD06 are within 50 hPa of each other, with MYD06 CTP tending to be a bit lower than CrIS. Over ocean, there are regions that display larger CTP differences, and these areas tend to have both high frequencies of low-level stratocumulus and low frequencies of cirrus. There is often optically thin cirrus overlying the low-level clouds in these regions. While this needs further exploration, the CrIS CTP seem to have a greater sensitivity to optically thin cirrus regardless of whether a lower-level cloud is present.

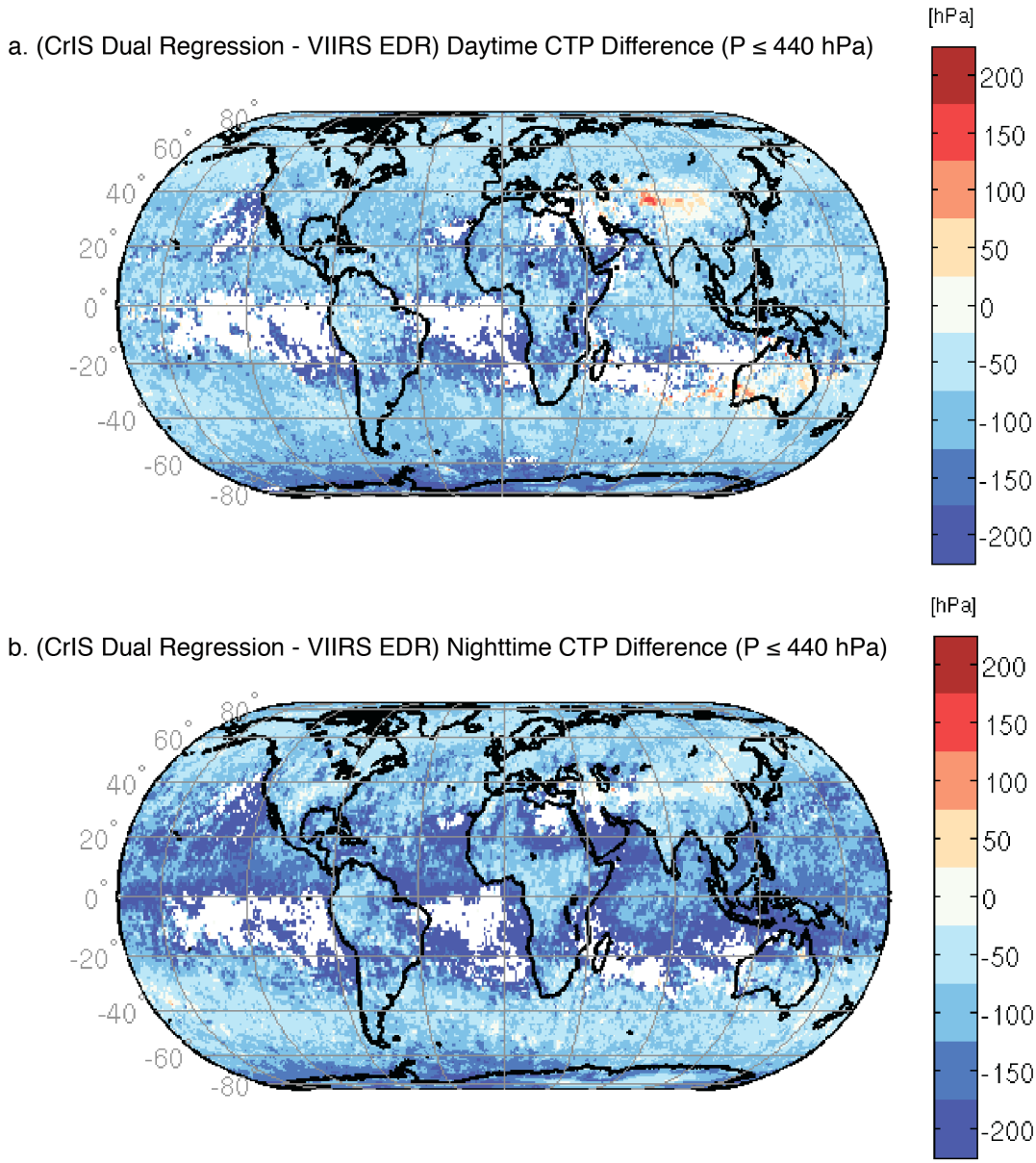

Fig. 5.2.1. Difference in high-level cloud top pressure (CTP) between the CrIS dual-regression method and the VIIRS EDR values for (a) daytime and (b) nighttime. Negative values (in blue) indicate that VIIRS CTPs generally have higher values than those from CrIS, which relate to lower cloud top heights.

While the cloud thermodynamic phase is not discussed in detail in this section, we suggest that it would be useful to transition the MODIS IR-phase algorithm (part of MOD06/MYD06) to VIIRS. While VIIRS does not have an absorbing infrared channel, a pseudo-channel could be provided by CrIS. An absorbing IR channel would greatly improve the inference of phase for optically thin ice clouds as shown in *Baum et al.* [2012]. Another issue with the MODIS method is that it requires a clear-sky radiance calculation, which in turn requires a radiative transfer model and atmospheric profiles of temperature, humidity, and ozone. The RT model used in the VIIRS EDRs is proprietary to the best of our knowledge, and should be updated to one that has heritage with the generation of global operational cloud products and that is freely available to the science community. One po-

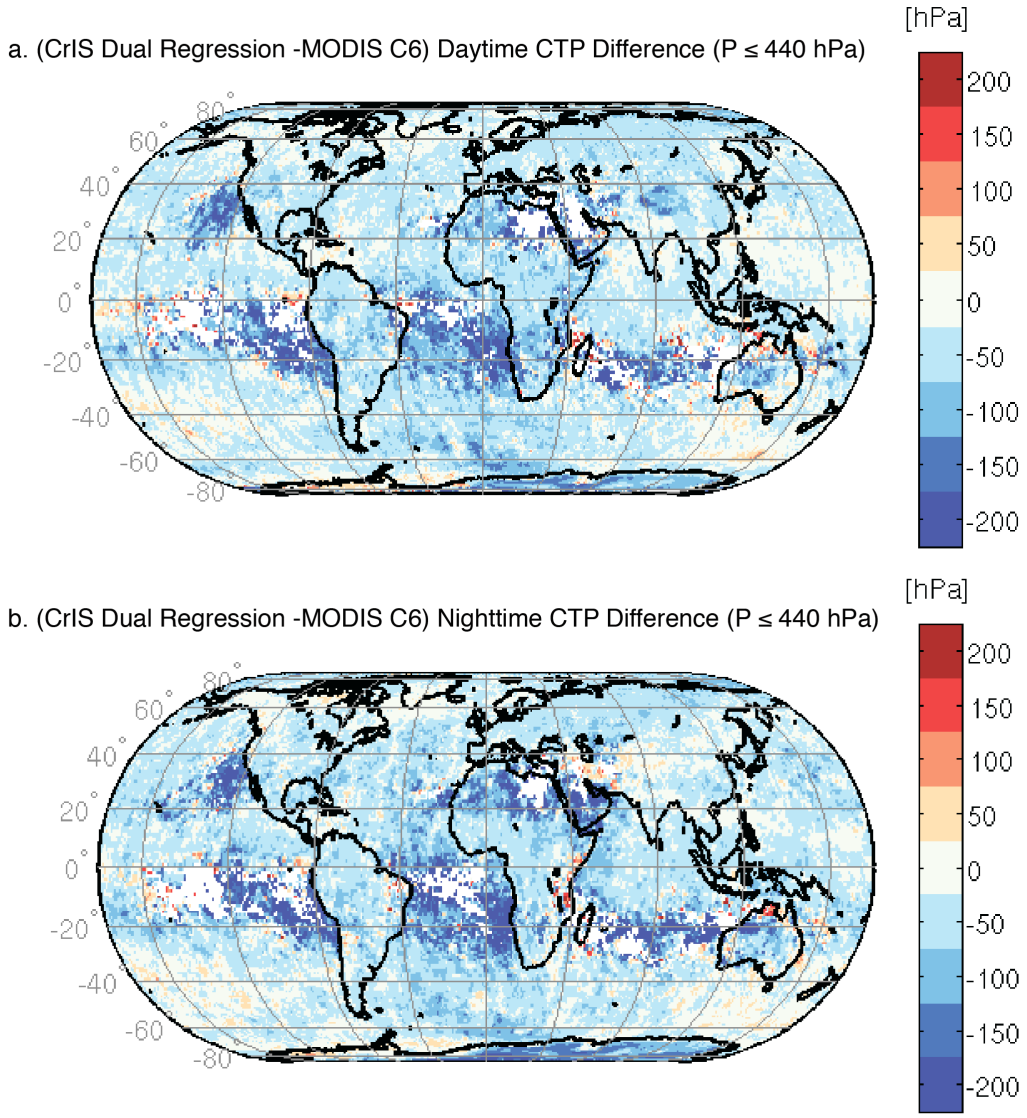

Fig. 5.2.2. Differences in high-level cloud top pressure between the CrIS dual-regression method and the MODIS Collection 6 MYD06 5 km CTP values for (a) daytime and (b) nighttime. Negative values (in blue) indicate that MYD06 CTPs generally have larger values than those from CrIS, which relate to lower cloud top heights. Note that for most of the globe, the CTP differences are within 50 hPa. There are regions over ocean that display higher CTP differences; these areas tend to have high frequencies of low-level stratocumulus and low frequencies of cirrus.

tential route is to adopt the Community Radiative Transfer Model (CRTM) as it has been developed to the point where it has specific routines for every polar-orbiting and geostationary imager and sounder that has been in orbit.

5.3 Development of Level-3 Gridded Products

The spatial and temporal aggregation of IDPS EDRs is not a Level-1 JPSS requirement despite the fact that the vast majority of science and application users require gridded statistics for their analysis. Without gridded aggregations (Level-3 products), the utility of even perfect algorithm continuity among Level-2 and EDR products is of little value for the model evaluation user community (e.g., IPCC CMIP5 assessments). This is a huge gap in the current JPSS algorithm design, and will severely limit the utility of the JPSS archived data for NASA climate science.

In order to enable continuation of NASA research and analysis climate efforts, it is imperative that NASA develop a pathway for gridding instantaneous pixel-level retrievals to weekly/monthly products. While a range of aggregation approaches (filtering, weighting, etc.) should be encouraged, a subset of the capability must include filtering that is consistent with the aggregation approaches adopted by EOS teams. That said, the EOS experience is that proper design of a Level-3 code is far from trivial. Statistics are affected by choices regarding aggregation strategies such as use of multiple orbits, daily-to-multiday weighting approaches, pixel weighting/filtering [*Maddux et al.*, 2010; *Pincus et al.*, 2012: *Stubenrauch et al.*, 2013]. Flexibility to quantify aggregation sensitivities to aggregation choices for individual sensors (or sensor combinations) is especially critical for building robust cloud climatologies.

By adopting similar aggregation strategies as used for the EOS legacy instruments, a set of JPSS aggregation products could be developed that would allow for a direct comparison against EOS gridded data records and potentially, a gridded data set that can potentially be used by the modeling and physical meteorological user community to bridge the EOS/NPP observation era.

In order to minimize additional resources needed to implement Sect. 5 recommendations, ESD is encouraged to explore and assess pathways that leverage existing instrument, algorithm and processing development efforts. Relevant funding sources are the Aqua/Terra Senior Review (supports MODIS Level-1 algorithm development, MODIS processing, etc.), ROSES (supports MODIS Level-2 and Level-3 algorithm refinement, as well as other cloud and A-Train algorithm-related activities), and the NPP line (supports VIIRS instrument characterization and the PEATEs).

6. Summary

The evaluation results provided in this report show that significant differences exist between VIIRS IP cloud masking, cloud-top and optical products and MODIS heritage products (MOD35, MOD06), as well as between the VIIRS products and retrievals from the team's hybrid GOES AWG/MODIS-like algorithm applied to VIIRS measurements

(VIIRS_AWGMOD). Specifically, there are extensive regions where serious biases are occurring between MODIS and VIIRS cloud top pressure, optical thickness, and effective particle size. The differences are significant in the sense of being orders of magnitude larger than the desired climate data record accuracies given by Ohring et al. [2005] for cloud studies (typically on the order of a couple of percent) or out of family with GEWEX cloud assessment data sets [*Stubenrauch et al.*, 2013] and the monthly annual cycle of other datasets (Sect. 1.6). The specific aggregation choices made in the generation of 5 km EDRs from the pixel-level IP products is unclear to the team; we have noted that EDR global CTP statistics are very sensitive to filtering with the data set's Quality Flags (QF). Consequently, the team has focused on IP products as they more more directly comparable with MODIS Level-2 products and algorithms.

Continuing geophysical data records across instrument sensors requires the use of common algorithms (including common forward radiative models, ancillary data, pixel filtering, etc.) in addition to having instruments with the same measurement capability or information content. As such, neither the VIIRS instrument nor the IDPS cloud algorithms will permit the continuation of the MODIS cloud top and optical/microphysical products. However, a common retrieval code that is limited to the same spectral channels available to both instruments provides an option for bridging the multi-instrument record (albeit at a lower quality than the more spectrally capable instrument alone). A version of such a code was developed for this report and run on VIIRS EDRs for the analysis month (referred to as VIIRS_AWGMOD) and used as a key means for evaluating the IDPS products.

Since JPSS requirements do not include the production of a gridded product, global statistical evaluations required the team to develop gridded aggregation codes that could be applied to IDPS cloud products, MODIS Collection 5 products from the LAADS archive (MOD35, MOD06), MODIS Collection 6 test products produced at the PEATE (MOD35_C6, MOD06_C6), and new team products produced at the PEATE (VIIRS_AWGMOD) or on team machines (CrIS_CTP_DR). The absence of JPSS temporal/spatial gridded products (i.e., Level-3 in NASA parlance) results in even adequate pixel-level geophysical products being of little value for the vast majority of users interested in analysis of cloud data records for climate studies.

Finally, even without the serious issues raised in this report regarding the VIIRS spectral coverage and IDPS products, the lack of an IDPS reprocessing capability makes such concerns a moot point with regard to climate data record generation. It is our experience that integration and use of the stand-alone ADL software is logistically problematic and cumbersome, and is not a work-around for NASA's processing needs. Further, IDPS algorithm codes are written in a manner specific to IDPS interfaces and therefore the porting of these codes to other processing systems will be challenging and time-consuming.

An overview of high-level conclusions and recommendations is given in the **Executive Summary**.

Appendix A. References

Journal References

Ackerman, S. A., K. I. Strabala, W. P. Menzel, R. A. Frey, C. C. Moeller, and L. E. Gumley Discriminating Clear-sky from Clouds with MODIS, 1998: *J. Geophys. Res.*, 103, D24, 32,141.

Ackerman, S. A., R. E. Holz, R. Frey, E. W. Eloranta, B. Maddux, and M. McGill, 2008: Cloud Detection with MODIS: Part II Validation, *JTECH*, 25, 1073-1086.

Baum, B. A., B. A. Wielicki, P. Minnis, and L. Parker, 1992: Cloud property retrieval using merged HIRS and AVHRR data. *J. Appl. Meteor.*, 31, 351-369.

Baum, B. A., P. Yang, A. J. Heymsfield, S. Platnick, M. D. King, Y. X. Hu, and S. T. Bedka, 2005: Bulk scattering properties for the remote sensing of ice clouds. 2: Narrowband models. *J. Appl. Meteor.*, 44, 1896-1911.

Baum, B. A., W. P. Menzel, R. A. Frey, D. Tobin, R. E. Holz, Ackerman, S. A., A. K. Heidinger, and P. Yang, 2012: MODIS cloud top property refinements for Collection 6. *J. Appl. Meteor. Clim.*, 51, 1145-1163.

Bony, S. and J.-L. Dufresne, 2005: Marine boundary layer clouds at the heart of tropical cloud feedback uncertainties in climate models. *Geophys. Res. Lett.*, 32, L20806, doi:10.1029/2005GL023851.

Dufresne, J.-L. and S. Bony, 2008: An Assessment of the Primary Sources of Spread of Global Warming Estimates from Coupled Atmosphere–Ocean Models, *J. Climate*, 21, 5135-5144, doi: 10.1175/2008JCLI2239.1.

Frey, R. A., S. A. Ackerman, Y. Liu, K. I. Strabala, H. Zhang, J. Key and X. Wang, 2008: Cloud Detection with MODIS, Part I: Recent Improvements in the MODIS Cloud Mask, *JTECH* **25**, 1057-1072.

Hanssen, A. W., and W. J. A. Kuipers, 1965: On the relationship between the frequency of rain and various meteorological parameters. *Meded. Verh.*, 81, 2–15.

Heidinger, A. K. and Pavolonis, M. J., 2009: Gazing at cirrus clouds for 25 years through a split window, part 1: Methodology. *J. Appl. Meteor. Climatology*, 48, 110-1116.

Heidinger, A. K., M. J. Pavolonis, R. E. Holz, B. A. Baum, and S. Berthier, 2010: Using CALIPSO to explore the sensitivity to cirrus height in the infrared observations from NPOESS/VIIRS and GOES-R/ABI. *J. Geophys. Res.*, 115, D00l15, doi:10.1029/2009JD012379.

Heidinger, Andrew K., Amato T. Evan, Michael J. Foster, Andi Walther, 2012: A Naive Bayesian Cloud-Detection Scheme Derived from CALIPSO and Applied within PATMOS-x. J. Appl. Meteor. Climatol., 51, 1129–1144.Holz, R.E., S. A. Ackerman, F.W. Nagle, R. Frey, R.E. Kuehn, S. Dutcher, M. A. Vaughan and B. Baum., 2008: Global MODIS Cloud Detection and Height Evaluation Using CALIOP. *J. Geophys. Res.*, doi:10.1029/2008JD009837.

Heidinger, A. K., R. Holz, A. Walther, D. Botambekov, S. Miller, C. Seaman, Y.-J. Noh, Q. Zhang, and B. A. Baum, 2012: JPPS Cloud Algorithm Assessment Report, prepared for the JPSS Project by the JPP Cloud Cal/Val team.

Holz, R.E. S. A. Ackerman, F.W. Nagle, R. Frey, R.E. Kuehn, S. Dutcher, M. A. Vaughan and B. Baum., 2008: Global MODIS Cloud Detection and Height Evaluation Using CALIOP. *J. Geophys. Res.*, doi:10.1029/2008JD009837.

Holz, R. E., et al., Finding closure between V3 CALIOP and MODIS optical depth retrievals using IR observations . *International Radiation Symposium*, Berlin Germany, August 2012.

Hutchison, K.D., Iisager, B. D., Kopp., T. J., and J. M. Jackson, (2008): "Discriminating between Clouds and Aerosols in the VIIRS Cloud Mask Algorithms," J. Atmospheric & Oceanic Technology, 25, 501-518.

Hutchison, K. D., and A. P. Cracknell, 2005: "VIIRS - A New Operational Cloud Imager," CRC Press, 218 pp.

Hutchison, K. D., Roskovensky, J. K., Jackson, J. M., Heidinger, A. K., Kopp, T. J., Pavolonis, M. J, and Frey, R., 2005: Automated Cloud Detection and Typing of Data Collected by the Visible Infrared Imager Radiometer Suite (VIIRS), *Int. J. Remote Sens.*, 20, 4681-4706.

King, M. D., W. P. Menzel, Y. J. Kaufman, D. Tanré, B. C. Gao, S. Platnick, S. A. Ackerman, L. A. Remer, R. Pincus, and P. A. Hubanks, 2003: Cloud and aerosol properties, precipitable water, and profiles of temperature and humidity from MODIS. *IEEE Trans. Geosci. Remote Sens.*, 41, 442-458.

King, M. D., S. Platnick, P. Yang, G. T. Arnold, M. A. Gray, J. C. Riédi, S. A. Ackerman, and K. N. Liou, 2004: Remote sensing of liquid water and ice cloud optical thickness and effective radius in the arctic: Application of airborne multispectral MAS data. *J. Atmos. Oceanic Technol.*, 21, 857-875.

King, M. D., S. Platnick, G. Wind, G. T. Arnold, and R. T. Dominguez, 2010: Remote sensing of radiative and microphysical properties of clouds during TC4: Results from MAS, MASTER, MODIS, and MISR. *J. Geophys. Res.*, 115, D00J07, doi:10.1029/2009JD013277.

King, M. D., S. Platnick, W. P. Menzel, S. A. Ackerman, and P. A. Hubanks: Spatial and Temporal Distribution of Clouds Observed by MODIS onboard the Terra and Aqua Satellites, *IEEE Trans. Geosci. Remote Sens.* (accepted Oct. 2012, scheduled to appear in print July 2013).

Maddux, B. C., S. A. Ackerman, and S. Platnick, 2010: Viewing geometry dependencies in MODIS cloud products, *J. Atmos. Oceanic Tech.*, 27, 1519–1528.

Menzel, W. P., R. Frey, H. Zhang, D. Wylie, C. Moeller, R. Holz, B. Maddux, B. A. Baum, K. Strabala, and L. Gumley, 2008: MODIS global cloud-top pressure and amount estimation: algorithm description and results. *J. Appl. Meteor. Climatol.*, 47, 1175-1198.

Moody, E. G., M. D. King, S., Platnick, C. B. Schaaf, and F. Gao, 2005: Spatially complete global spectral surface albedos: Value-added datasets derived from Terra MODIS land products. *IEEE Trans. Geosci. Remote Sens.*, 43, 144-158.

Moody, E. G., M. D. King, C. B. Schaaf, D. K. Hall, and S. Platnick, 2007: Northern hemisphere five-year average (2000-2004) spectral albedos of surfaces in the presence of snow: Statistics computed from Terra MODIS land products. *Rem. Sens. Env.*, 111, 337-345.

Moody, E. G., M. D. King, C. B. Schaaf, and S. Platnick, 2008: MODIS-derived spatially complete surface albedo products: Spatial and temporal pixel distribution and zonal averages. *J. Appl. Meteor. Climatol.*, 47, 2879–2894.

Nakajima, T., and M. D. King, 1990: Determination of the optical thickness and effective particle radius of clouds from reflected solar radiation measurements, Part I: Theory. *J. Atmos. Sci.*, 47, 1878-1893.

Nagle, Frederick W. and Holz, Robert E., 2009: Computationally efficient methods of collocating satellite, aircraft, and ground observations. *J. Atmos. Oceanic Tech.*, 26, issue 8, pp.1585-1595.

Ohring, G., et al., 2005: Satellite Instrument Calibration for Measuring Global Climate Change: Report of a Workshop. *BAMS*, doi:10.1175/BAMS-86-9-1303.

Pincus, R., S. Platnick, S. A. Ackerman, R. S. Hemler, R. J. P. Hofmann, 2012: Reconciling simulated and observed views of clouds: MODIS, ISCCP, and the limits of instrument simulators. *J. Climate*, doi: 10.1175/JCLI-D-11-00267.1.

Platnick, S., and F. P. J. Valero, 1995: A validation study of a satellite cloud retrieval during ASTEX. *J. Atmo. Sci.*, 52, 2985-3001.

Platnick, S., M. D. King, S. A. Ackerman, W. P. Menzel, B. A. Baum, J. C. Riédi, and R. A. Frey, 2003: The MODIS cloud products: Algorithms and examples from Terra. *IEEE Trans. Geosci. Remote Sens.*, 41, 459-473.

Platnick, S., R. Pincus, B. Wind, M. D. King, M. Gray, P. Hubanks, 2004: MODIS cloud optical thickness and effective particle size retrievals. Passive Optical Remote Sensing of the Atmosphere and Clouds IV, Eds., S.-C. Tsay, T. Yokota, M.-H. Ahn, *Proc. of SPIE*, Vol. 5652, doi: 10.1117/12.578353.

Platnick, S., J. Gleason, P. Sellers, et al.: White Paper on Continuity of NASA Satellite Climate and Earth Science Data Records into the NPP/JPSS-1 Era. Document to NASA HQ Earth Science Division, November 2011.

Platnick, S., N. Amarasinghe, P. Hubanks: "MODIS Atmosphere Products: The importance of record quality and length in quantifying trends and correlations", plenary presentation at MODIS Science Team Meeting, College Park, MD, May 2011, http://modis.gsfc.nasa.gov/sci_team/meetings/201105/plenary.php.

Rossow, W. B., A. W. Walker, and L. C. Gardner, 1993: Comparison of ISCCP and other cloud amounts, *J. Climate*, 6:2394-2418.

Smith, N., W. P. Menzel, E. Weisz, A. Heidinger, and B. A. Baum, 2013: A uniform space-time grid for comparison of global satellite cloud products: Characterization and sensitivity studies. *J. Appl. Meteor. Clim.,* 52, 255-268.

Smith, W. L., E. Weisz, S. V. Kireev, D. K. Zhou, Z. Li and E. E. Borbas, 2012: Dual regression retrieval algorithm for real-time processing of satellite ultraspectral radiances. *J. Appl. Meteor. Clim.*, **51**, 1455-1476.

Stubenrauch, C. J., W. B. Rossow, S. Kinne, S. Ackerman, G. Cesana, H. Chepfer, B. Getzewich, L. Di Girolamo, A. Guignard, A. Heidinger, B. Maddux, P. Menzel, P. Minnis, C. Pearl, S. Platnick, C. Poulsen, J. Riedi, S. Sun-Mack, A. Walther, D. Winker, S. Zeng, and G. Zhao, 2013: Assessment of global cloud datasets from satellites: Project and database initiated by the GEWEX Radiation Panel. *Bull. Am. Meteor. Soc.*

Tiao, G.C., Reinsel, G.C., Xu, D., Pedrick, J.H., Zhu, X., Miller, A.J., DeLuisi, J.J., Mateer, C.L. and Wuebbles, D.J. (1990). Effects of autocorrelation and temporal sampling schemes on estimates of trend and spatial correlation. *J. Geophys. Res.,* 95(D12), doi: 10.1029/90JD01305. issn: 0148-0227.

Thomas, S. M., A. K. Heidinger, and M. J. Pavolonis, Comparison of NOAA's operational AVHRR-derived cloud amount to other satellite-derived cloud climatologies. Journal of Climate, Volume 17, Issue 24, 2004, pp.4805-4822. Call Number: Reprint 3992.

Wang, M., and M. D. King, 1997: Correction of Rayleigh scattering effects in cloud optical thickness retrievals. *J. Geophys. Res*, 102, 25915-25926.

Weatherhead, E. C., G. C. Reinsel, G. C. Tiao, X.-L. Meng, D. Choi, W.-K. Cheang, T. Keller, J. DeLuisi, D. J. Wuebbles, J. B. Kerr, A. J. Miller, S. J. Oltmans, and J. E. Federick, 1998: Factors affecting the detection of trends: Statistical considerations and applications to environmental data records, *J. Geophys. Res.*, 103, 17149-17161.

Webb, M., F. Lambert, and J. Gregory, 2013: Origins of differences in climate sensitivity, forcing and feedback in climate models. *Clim. Dynamics*, 40, 677–707, doi: 10.1007/s00382-012-1336-x.

Weisz, E., W. P. Menzel, N. Smith, R. Frey, E. E. Borbas, and B. A. Baum, 2012: An approach for improving cirrus cloud top pressure/height estimation by merging high spatial resolution infrared window data with high spectral resolution sounder data. *J. Appl. Meteor. Clim.*, 51, 1477-1488.

Wind, G., S. Platnick, M. D. King, P. A. Hubanks, M. J. Pavolonis, A. K. Heidinger, B. A. Baum, and P. Yang, 2010: Multilayer cloud detection with the MODIS near-infrared water vapor absorption band, *J. Appl. Meteor. Climatology*, 49, 2315-2333.

Winker, D. M., W. H. Hunt, and M. J. McGill, 2007: Initial performance assessment of CALIOP. *Geophys. Res. Lett.*, 34, L19803. doi:10.1029/2007GL030135.

Wong, E., Hutchison, K.D., Ou, S.C., and K. N. Liou, 2007: Cirrus cloud top temperatures retrieved from radiances in the National Polar-Orbiting Operational Environmental Satellite System-Visible Infrared Imager Radiometer Suite 8.55 and 12.0 μm bandpasses, *Appl. Opt.,* 46, 1316-1325.

Wylie, D. P., W. P. Menzel, H. M. Woolf, and K. I. Strabala, 1994: Four years of global cirrus cloud statistics using HIRS. *J. Climate,* 7, 1972-1986.

Yang, P., L. Zhang, G. Hong, S. L. Nasiri, B. A. Baum, H.-L. Huang, M. D. King, and S. Platnick, 2007: Differences between collection 004 and 005 MODIS ice cloud optical/microphysical products and their impact on radiative forcing simulations, *IEEE Trans. Geosci. Remote Sens.*, 45, 2886-2899.

Zelinka, M. D., S. A. Klein, and D. L. Hartmann, 2012a: Computing and partitioning cloud feedbacks using cloud property histograms. Part I: Cloud radiative kernels. *J. Climate*, 25, 3715-3735.

Zelinka, M. D., S. A. Klein, and D. L. Hartmann, 2012b: Computing and partitioning cloud feedbacks using cloud property histograms. Part II: Attribution to changes in cloud amount, altitude, and optical depth. *J. Climate*, 25, 3736-3754.

Zelinka, M.D., S.A. Klein, K.E. Taylor, T. Andrews, M.J. Webb, J.M. Gregory, and P.M. Forster, 2013: Contributions of Different Cloud Types to Feedbacks and Rapid Adjustments in CMIP5. In press, *J. Climate*. doi: 10.1175/JCLI-D-12-00555.1

Zhang, Z., S. Platnick, P. Yang, A. Heidinger, and J. M. Comstock, 2010: Effect of ice particle size vertical inhomogeneity on the passive remote sensing of ice clouds, *J. Geophys. Res.*, 115, 16 pp., doi:10.1029/2010JD013835.

Other References

Baum, B. A., S. Ackerman, L. Gumley, A. Heidinger, R. Holz, M. D. King, W. P. Menzel, S. Platnick, H. Revercomb, and P. Yang: *White Paper on NASA Alternatives to NGAS Cloud Products from NPP/NPOESS*, 7 pp., April 9, 2010.

JPSS Level 1 Requirements Supplement 2.0, NOAA/NESDIS, 122 pp., 16 September 2012.

Heidinger, A., R. Holz, A. Walther, D. Botambekov, S. Miller, C. Seaman, Y.-J. Noh, Q. Zhang, and B. Baum: *JPSS Cloud Algorithm Assessment Report*. Document to JPSS Project from the JPSS Cloud Cal/Val Team, 27 December 2012.

JPSS ATBD and OAD documents available from the NASA Suomi NPP web site: http://npp.gsfc.nasa.gov/science/documents.html.

MODIS Atmosphere Team web site: http://modis-atmos.gsfc.nasa.gov.

MODIS Atmosphere Team C6 documentation: http://modis-atmos.gsfc.nasa.gov/products_C006update.html, and links to product test imagery: http://modis-atmos.gsfc.nasa.gov/team/index.html.

Platnick, S., J. Gleason, P. Sellers, et al.: *White Paper on Continuity of NASA Satellite Climate and Earth Science Data Records into the NPP/JPSS-1 Era*. Document to NASA ESD, 60 pp., November 2011.

Wong, E. and P. D. Siebels. OPERATIONAL ALGORITHM DESCRIPTION DOCUMENT FOR VIIRS CLOUD COVER/LAYERS (CCL) AND GENERATE CLOUD EDR (D39590 Rev A), 54 pp., 2009a.

Wong, E. and P. D. Siebels. OPERATIONAL ALGORITHM DESCRIPTION DOCUMENT FOR VIIRS CLOUD OPTICAL PROPERTIES (COP) SOFTWARE (D39298 Rev A), 32 pp., 2009b.

Appendix B. Overview of Suomi NPP Cloud Team Objectives and Activities

Table B.1. Overview and current status of NPP cloud team objectives. IDPS, MODIS, and team products are shown in bold-face with an explanation provided following the table. The overall goal is to evaluate the potential for VIIRS and CrIS SDR data records to continue the EOS/MODIS cloud data records. This is being done by: (1) Direct evaluation of VIIRS EDRs against collocated MODIS and A-Train data; (2) Porting of GOES AWG and MODIS-like algorithms to the VIIRS SDRs; (3) Investigating use of CrIS observations to improve cloud top property skill lost due to the absence of VIIRS CO_2 slicing channels.

Atmospheres Team: Overview of SDRs, PEATE Activities, and Cloud EDRs			
Category	**Product/Activity**	**Investigation Leads**	**Description**
A. VIIRS SDR Evaluation	Solar Reflectance Bands	N/A	Not part of funded investigation team proposals.
	Thermal Emissive Bands	N/A	
B. Co-location of relevant NPP, Aqua, and CALIPSO data sets	VIIRS/MODIS	PEATE, Holz	Merged (aka, match-up) data sets archived at the Atmosphere PEATE
	VIIRS/CALIOP, MODIS/CALIOP	PEATE, Holz	Merged data sets archived at the Atmosphere PEATE
	VIIRS/CrIS, MODIS/AIRS	PEATE, Holz	Merged data sets archived at the Atmosphere PEATE
C. VIIRS Cloud EDR Evaluation or Related	VIIRS Cloud Mask (**VCM**) evaluation	Ackerman	Evaluation against MODIS (**MOD35**) and CALIOP. VCM includes cloud phase.
	VIIRS Cloud Top Properties evaluation (**CTT**, **CTP**, **CTH**)	Heidinger, Baum	Evaluation against CALIOP, MODIS (**MOD06_C5, MOD06_C6**), and VIIRS GOES-AWG product (see below).
	VIIRS Cloud Optical Properties evaluation (**COT**, **CER**)	Platnick, Holz	Evaluation against MODIS (**MOD06_C5, MOD06_C6**) and MODIS-like VIIRS product (see below).
	VIIRS Cloud Base Height evaluation (**CBH**)	N/A	Not part of funded investigation team proposals. Not an EOS continuity data record.
	Ice Cloud LUT evaluation	Yang, Nasiri	Comparison against MODIS C5 and C6 ice radiative models.
D. New Cloud Algorithms and other Data Set Development	Development of a common cloud mask for VIIRS and MODIS based on MOD35 (**VIIRS_VMCM, MODIS_VMCM**)	Ackerman	Allow for like comparisons. Excludes CO_2 and/or water vapor channels not available on VIIRS. Not required for report evaluation. Status: On-going. Scheduled for completion in spring 2013.

	Development of a common GOES AWG-like cloud top properties algorithm for VIIRS (**VIIRS_AWGMOD**) and MODIS (**MODIS_AWGMOD**).	Heidinger	Allows for like comparisons using the same common spectral information available from VIIRS and MODIS. Status: VIIRS_AWGMOD being processed and archived on the Atmosphere PEATE on an ongoing basis. MODIS_AWGMOD processing on PEATE is in test phase.
	Development of a common MODIS-like cloud optical properties algorithm (based on Collection 6 MOD06) for VIIRS (**VIIRS_AWGMOD**) and MODIS (**MODIS_AWGMOD**). Uses input from AWG cloud-top algorithm which is included in the product.	Platnick	Allows for like comparisons using the same common spectral information available from VIIRS and MODIS. Status: VIIRS_AWGMOD being processed and archived on the Atmosphere PEATE on an ongoing basis. MODIS_AWGMOD PEATE processing is in test phase.
	CrIS cloud top properties (**CrIS_CTP_DR**)	Baum, Menzel, Weisz	"Dual Regression" algorithm. Status: Retrievals for the cloud team's golden month (Sept. 2012) has been processed for AIRS, CrIS, and IASI outside of the PEATE. Plan is to integrate into Atmosphere PEATE in January 2012 timeframe. Goal is to eventually merge imager + sounder retrievals using MODIS+AIRS (Aqua), AVHRR+IASI (MetOp-A) and VIIRS+CrIS (NPP) instrument pairs.
	CrIS cloud top properties (**CrIS_CTP_FOV**)	Holz, Platnick	Apply MOD06 CO_2 slicing algorithm to CrIS FOVs for use in CTP and COP code. Status: Task will not begin until after evaluation report completed.
	Development of L3 aggregation code	Baum/Smith [1], Holz) [2]	[1] Space Time Gridding (STG) software developed by team for use with CrIS and/or VIIRS cloud-top property aggregations. [2] Used for cloud mask, cloud-top and optical properties. Status: completed.
	Development of VIIRS L1B file format that is common with MODIS (for use by aerosol and cloud team)	PEATE	Generate common VIIRS L1B file format that can assist cloud/aerosol team in porting MODIS-like code to VIIRS, ensure all team members are using same SDR calibration/version, and serve as a pathway to evaluation and/or data record continuity. Status: completed.

Appendix C. Key Acronyms

ADL: Algorithm Development Library

C5: Collection 5 MODIS atmosphere team processing stream (version), begun in mid-2006

C6: Collection 6 MODIS atmosphere team processing stream (version), expected to begin in early 2013

CBH: Cloud Base Height

CrIS_CTP_DR: a CrIS algorithm for cloud-top properties developed by team members using the dual-regression approach of *Weisz et al.* [2012]

CrIS_CTP_FOV: a CrIS algorithm for cloud-top properties developed by team members using individual CrIS FOVs that is being planned for integration into the VIIRS_AWGMOD code.

CER: Cloud Effective particle Radius

CLASS: Comprehensive Large Array-Data Stewardship System (NOAA archive facility)

COP: Cloud Optical Properties

COT: Cloud Optical Thickness

CREW: Cloud Retrieval Evaluation Workshops (sponsored by Eumetsat)

CTH: Cloud Top Height

CTP: Cloud Top Parameters (JPSS nomenclature for suite of cloud top products) or Cloud Top Pressure

CTT: Cloud Top Temperature

GEWEX Cloud Assessment: Global Energy and Water Cycle Experiment (under WCRP) cloud assessment report, finalized in 2012

GOES-R AWG: NOAA Algorithm Working Group cloud code for the GOES-R ABI imager, similar to PATMOS-x code

MODIS_AWGMOD: a common VIIRS/MODIS cloud retrieval code developed by the team from heritage GOES-R AWG and MODIS MOD06 algorithms and applied to MODIS L1B data

MODIS_VMCM: a common VIIRS/MODIS cloud mask developed by team members and applied to MODIS L1B data

MOD06: MODIS cloud top and optical/microphysical Level-2 product file ID

MOD35: MODIS cloud mask Level-2 product file ID

PATMOS-x: Pathfinder Atmospheres - Extended for AVHHR; similar to GOES-R AWG code

VCM: VIIRS Cloud Mask

VIIRS_AWGMOD: a common VIIRS/MODIS cloud retrieval code developed by the team from heritage GOES-R AWG and MODIS MOD06 algorithms and applied to VIIRS SDRs

VIIRS_VMCM: a common VIIRS/MODIS cloud mask developed by team members and applied to VIIRS SDRs